

Review

# A Review on Fabrication of Cylindrical and Rotating Parts by Thermoelectric-Erosion Based Turning Processes

Sujeet Kumar Chaubey  and Kapil Gupta \* 

Department of Mechanical and Industrial Engineering Technology, University of Johannesburg, Doornfontein, Johannesburg 2028, South Africa; schaubey@uj.ac.za

\* Correspondence: kgupta@uj.ac.za

**Abstract:** Nowadays, advanced turning processes are extensively being adopted to perform different types of turning operations such as straight turning, taper turning on Hastelloy, Nimonic, and Inconel, stainless steel, and tool steel to fabricate better quality cylindrical and rotating parts such as miniature-bars, miniature-pins, miniature-electrodes, and miniature-tools. This paper presents a review of the previous research conducted on the turning of miniature cylindrical bars using thermoelectric-erosion based turning processes namely thermoelectric-erosion turning (TET) and wire-assisted thermoelectric-erosion turning (WTET). It also highlights work and tool electrode materials, types of dielectrics, detailed specifications of turning, types of turning, process parameters, performance measures, advantages and limitations, and key findings. The paper ends with conclusions and future research directions. This paper aims to facilitate researchers and scholars by highlighting the potential and capabilities of TET and WTET processes and providing relevant information for ease of fabrication of miniature parts and components from a wide range of difficult-to-machine materials.

**Keywords:** difficult-to-machine materials; miniature parts; steel; thermoelectric-erosion; turning



**Citation:** Chaubey, S.K.; Gupta, K. A Review on Fabrication of Cylindrical and Rotating Parts by Thermoelectric-Erosion Based Turning Processes. *Metals* **2022**, *12*, 1227. <https://doi.org/10.3390/met12071227>

Academic Editor: Thomas Fiedler

Received: 3 June 2022

Accepted: 18 July 2022

Published: 20 July 2022

**Publisher's Note:** MDPI stays neutral with regard to jurisdictional claims in published maps and institutional affiliations.



**Copyright:** © 2022 by the authors. Licensee MDPI, Basel, Switzerland. This article is an open access article distributed under the terms and conditions of the Creative Commons Attribution (CC BY) license (<https://creativecommons.org/licenses/by/4.0/>).

## 1. Introduction

The demand for cylindrical and rotating structures/parts, having spatial rotary surfaces, as shown in Figure 1, is increasing very rapidly and consistently due to their wide applications in space, biomedical, precision scientific, and instrumentation industries [1–3]. The cylindrical and rotating structures/parts used for aforesaid applications are fabricated from difficult-to-machine materials such as advanced materials, superalloys, titanium alloys, cemented carbides, Hastelloy, Nimonic, Inconel, stainless steel, tool steel, and polycrystalline diamonds. Turning is the most commonly used and basic machining operation in the manufacturing industries to fabricate the different types of rotary parts and structures on rotating cylindrical bars made from a variety of materials [4]. Turning of cylindrical bars to fabricate cylindrical structures/parts having a diameter less than 1 mm (i.e.,  $\phi < 1000 \mu\text{m}$ ) is known as micro-sized turning [5]. Whereas, if the diameter ranges between 1 to 10 mm, then it is referred to as meso-sized turning. But, the conventional turning of cylindrical bars is challenging with certain dimensional accuracy and surface quality constraints [6–8]. It draws the attention of researchers, engineers, and industrial users to explore alternative manufacturing processes to produce high-aspect-ratio micro and meso-sized cylindrical and rotating parts from difficult-to-machine materials. Non-contact or advanced machining has the potential to fabricate cylindrical and rotating parts from a wide range of difficult-to-machine materials, having diameters in a range of a few microns to hundreds of microns, with better dimensional accuracy and surface finish [6–8].

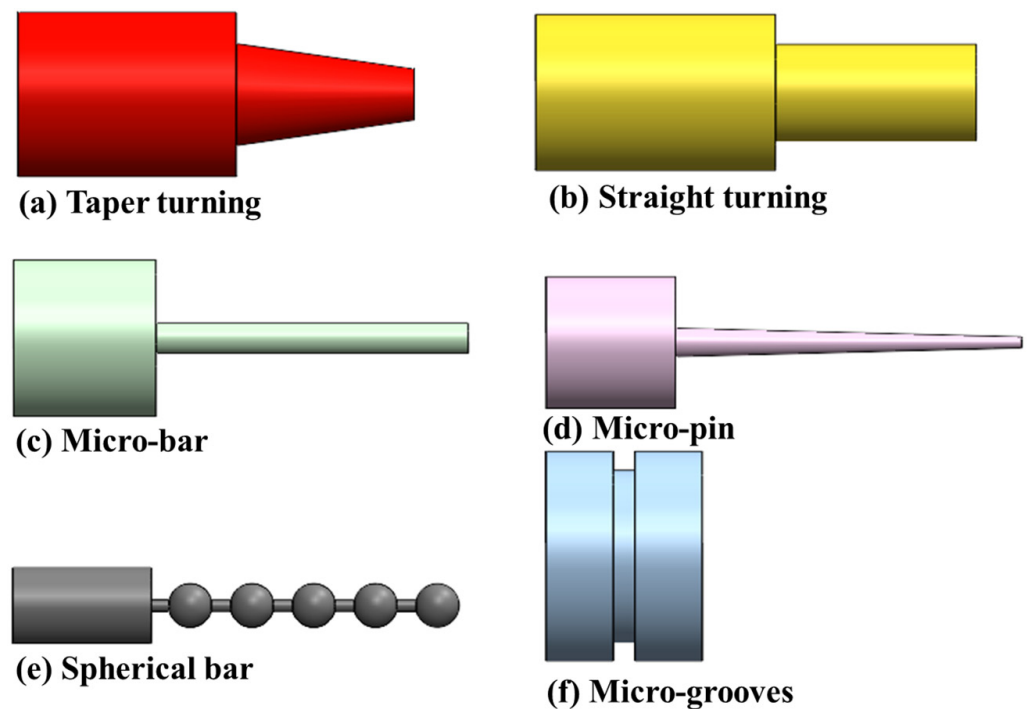


**Figure 1.** Schematic representation of turning process types and range of parts made by them: (a) Taper turning; and (b) Straight turning; (c) high-aspect-ratio micro-bar; (d) high-aspect-ratio micro-pin; (e) spherical bar; and (f) micro-grooves.

### 1.1. Selection of Materials for Turning Operation

Types of materials for turning cylindrical and rotating parts are based on the end-user application. While, the selection of turning methods depends on the types of material and their characteristics (i.e., hardness stiffness, and strength). Usually, different types of turning operations such as straight turning, taper turning, and grooving are performed on various metallic, non-metallic, composites, and advanced materials. Metallic materials may be ferrous or non-ferrous. Ferrous materials such as stainless steel, high carbon, high-speed steel, and cast steel have higher strength than non-ferrous metals (i.e., copper, aluminum, lead, zinc, brass, nickel, and their alloys) and are most suitable for various heavy industrial applications [9,10]. Delrin, polyvinyl chloride, acrylic, fiberglass, nylon, etc. are non-metallic materials and are popularly referred to as plastics having lightweight and noiseless properties and mostly used in several home appliances and toys. Composite materials such as ceramic matrix composite, metal matrix composite, glass fiber reinforced composite, fiberglass, and carbon fiber reinforced polymer, are a mixture of two or more individual materials of different physical and chemical properties. These materials are widely used in aerospace, automotive, marine, and electrical applications due to their lightweight, high strength, stiffness, and electrical resistance. Cylindrical parts of some advanced materials such as high strength and temperature alloys, bio and smart materials, refractory materials, high-performance composites, etc. are also used for specialized applications. Table 1 presents the characteristics, features, and specific applications of different important materials used by previous researchers to make cylindrical and rotating parts using TET and WTET processes.

**Table 1.** Characteristics, features, and applications of different materials used in TET and WTET [10].

Material Type	Characteristics	Features and Applications
Stainless steel	High corrosion resistance, non-magnetic, non-hardenable	Medical industries, aircraft, automotive, and food industries
Inconel	Resistant to corrosion and extreme temperatures, and high mechanical strength	Gas turbine, aerospace, and aircraft parts
Tool steel	High strength, extreme hardness, and resistance to wear	Dies, punch, blanking tools, and gauges
Die steel	Excellent wear and abrasion-resistant properties	Tools, dies, and instruments
Shape memory alloys	React to changes in their environment and ability to regain their original shape	Micro-valves, actuators, and biomedical applications
Titanium alloys	Higher strength to weight ratio, corrosion-resistant	For lightweight and low-strength applications
Aluminum alloys	Lightweight, non-corrosive, excellent machinability	For extremely light-duty instruments and for high precision applications
Bronze alloys	Excellent machinability, low friction, good compatibility	For high-precision applications
Sintered powdered alloys	Low cost, low quality, moderate strength	For commercial applications
Metal matrix composites	High-temperature resistance	Carbide drills, aircraft components, automotive industries

### 1.2. Methods of Turning Cylindrical Bars

Table 2 presents the summary of various methods of machining to perform straight turning, taper turning, and grooving on cylindrical bars to fabricate cylindrical structures such as miniature-pins, -tools, etc. Methods of machining these cylindrical structures can be categorized as (i) contact type or traditional turning methods; (ii) micro-manufacturing processes, and (iii) non-contact type or advanced turning methods [10].

Lathe and milling and their micro-versions are the most commonly used contact type turning methods to produce miniature-sized cylindrical structures on metallic and non-metallic materials with the help of the single-point cutting tool and milling cutter. These turning methods are always associated with some inherent limitations such as work materials, complex geometrical shape, special tooling requirements, tool wear, burr formation, poor edge definition, dimensional inaccuracy, and poor surface quality [11]. Lithography, electroplating, and molding (LIGA), powder metallurgy (PM), powder injection molding (PIM), micro etching, and laser processing are micro-manufacturing processes to fabricate microstructures. These micro-manufacturing processes have also some drawbacks such as being expensive, the requirement of X-ray (LIGA) and molds (PIM), porosity (PM), and being suitable for non-reflective materials (Laser) [10].

**Table 2.** Commonly used turning methods to fabricate different types of cylindrical parts.

Type	Methods	Nature of the Process	Manufacturing Process
Contact type or Traditional turning methods	Chip formation	Subtractive (Lathe)	<ul style="list-style-type: none"> <li>Conventional lathe, CNC-Lathe, Micro-lathe, CNC-milling, and their micro-versions</li> </ul>
Micro-manufacturing processes	Formative	Additive or accretion	<ul style="list-style-type: none"> <li>Lithography, electroplating, and molding (LIGA)</li> <li>Powder metallurgy (PM),</li> <li>Powder injection molding (PIM),</li> </ul>
		Chemical ablation	<ul style="list-style-type: none"> <li>Chemical etching</li> </ul>
	Melting and vaporization	Thermoelectric vaporization	<ul style="list-style-type: none"> <li>Laser processing</li> </ul>
Non-contact type or Advanced turning methods	Thermoelectric-erosion based turning	Controlled spark erosion	<ul style="list-style-type: none"> <li>TET, WTET and its variants</li> </ul>

Due to the aforementioned limitations, non-contact type methods are being adopted to fabricate cylindrical structures on various materials. Non-contact types or advanced processes for turning are modified thermoelectric-erosion based machining processes such as thermoelectric-erosion turning (TET), wire-assisted thermoelectric-erosion turning (WTET), and Hybrid WTET [12]. These processes offer a feasible approach for the fabrication of cylindrical parts due to their machining characteristics such as precise and cost-effective, non-contact type nature, and free from cutting force during machining of metals and alloys [13,14]. In thermoelectric-erosion based turning processes, the excess materials from a cylindrical workpiece are removed by the means of generating a series of repetitive electrical sparks between tool electrodes and the rotating cylindrical workpiece [15]. TET and WTET are unique modifications of thermoelectric-erosion based machines (TEM) to fabricate high aspect ratio cylindrical parts by adding a rotary set up on the working table of conventional TEM which served as an additional rotational axis. Many researchers have developed different types of rotary setups for TET and WTET and worked on different aspects of turning to improve the developed processes [16]. The schematic diagram of a TET and WTET process is shown in Figure 2. The major advantages of these processes are (i) the ability to fabricate high aspect ratio miniature parts, (ii) the ability to perform turning on any kind of materials regardless of their hardness such as titanium alloys and metal matrix composites (MMC), (iii) ability to form turning on thin and fragile materials; (iv) no burr and sharp edge formation, (v) produce the better quality turned surfaces free from crack and voids, mechanical stresses, cutting forces, deformation, chatter, and vibration errors due to non-contact nature, and (vi) unattended operation [17,18]. Apart from this, WTET is an eco-friendly process because it uses deionized water as a dielectric. Furthermore, WTET uses the same fine wire as a tool electrode to perform all kinds of turning operations.

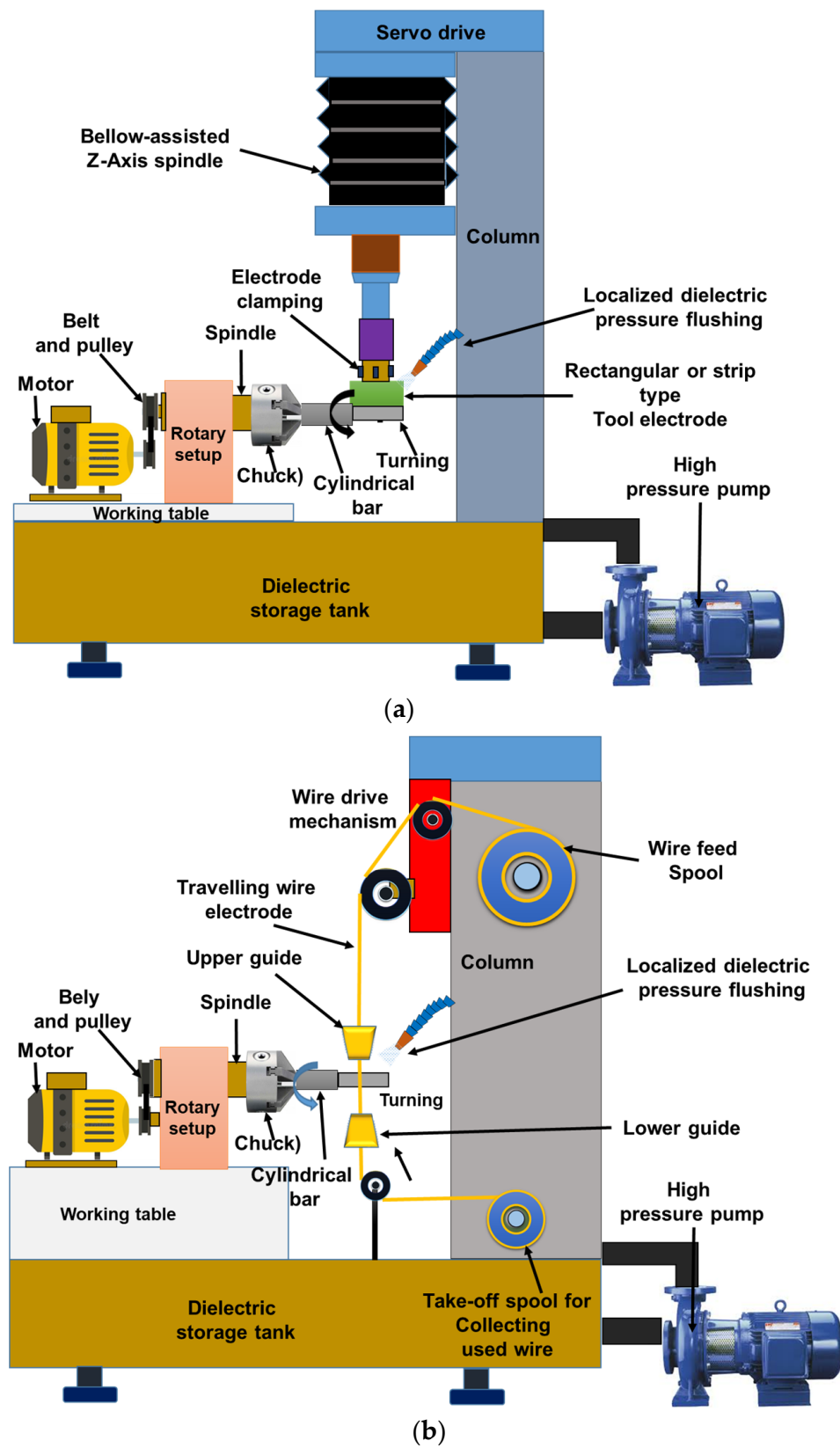


**Figure 2.** Schematic representation of wire-assisted thermoelectric-erosion based turning setup: (a) thermoelectric-erosion turning (TET) process; and (b) wire-assisted thermoelectric-erosion turning (WTET) process.

The additional rotary setup in thermoelectric erosion-based turning processes moves along the X and Y axis with the movement of the working table in the same directions to perform the turning operation [19]. The separate power supply is given to the motor which rotates the spindle attached with chuck or collet at desired speed with the help of the controller/varying the voltage (in case of servo and stepper motor) or by changing the frequency (in case of an induction motor). The speed of the workpiece can be controlled by varying the frequency of the supply (in the case of an induction motor) or by varying the supply voltage or controller (in the case of servo and stepper motor) or by changing the driven pulley. The working principle, mechanism of material removal, and additional rotary setup attachment are the same for TET and WTET processes. Only, tool electrodes and types of dielectric are the major difference between these two processes. While the functions of dielectrics are the same in both TET and WTET processes. In TET, fabricated tool electrodes (rectangular strip or strip electrode) made of brass or copper are used to form a negative image on a rotating workpiece in the presence of continuously flowing dielectric such as EDM oil, kerosene, or hydrocarbons to remove the eroded particles from the interelectrode-gap (IEG) to minimize the formation of eroded particles on turned surfaces and ensure smooth turning without short-circuiting [17]. The strip electrode is firmly held with the help of a tool holder and can be moved upward and downward directions along Z-axis to perform a turning operation. The constant gap between the strip electrode and the cylindrical workpiece is maintained with the help of a servo motor. In TET, the tool electrode and workpiece are submerged in the dielectric during the turning process. Nowadays, the WTET process is widely used to perform various turning operations to fabricate cylindrical structures. In this process [20], a continuous traveling (vertically or horizontally) fine wire having a diameter ranging between 0.1–0.25 mm is used as a tool electrode to perform the turning of a rotating cylindrical bar firmly hold by a chuck and rotate with the help of a motor and belt-driven rotary arrangement to fabricate cylindrical parts. Usually, deionized water is used to flush away the eroded particles known as debris from IEG. In WTET, localized flushing is used with the help of both guides. Wire tension is maintained between the two-wire guides to avoid wire vibration during turning. The lower guide is fixed while the upper guide can move upward or downward along Z-axis with the help of a servo motor. The mechanism of material removal is based on thermoelectric-erosion. A very strong electric field is formed at minimum IEG after supplying DC power to the tool electrode and rotating workpiece. The suspended microscopic particles in a dielectric fluid are accumulated around the location of the strongest electric field and form a conductive bridge across the electrodes gap. When the supply voltage is exceeded to dielectric breakdown voltage, the conductive bridge breaks due to excessive heat and temperature. Due to the collapse of the conductive bridge sparks are generated between the electrodes gap. The material is removed from the workpiece due to melting and vaporization and at the same time dielectric is flushed away from the eroded particles from the electrodes gap to ensure smooth drilling. The generation of sparks is continuously repeated till turning up to the desired length [21].

The wire-assisted thermoelectric-erosion based turning process is mostly used to fabricate high-quality cylindrical parts by various turning operations such as straight turning, taper turning, and grooving [1,16,19]. These cylindrical parts fabricated by WTET are used in several industrial applications such as aerospace, bio-implants, automotive industries, and micro-electromechanical systems (MEMS). The products and components fabricated by these processes are: (i) miniature-bars; (ii) miniature-pins; (iii) miniature-tools; (iv) miniature-electrodes; and (v) miniature-probes etc.

### *1.3. Process Parameters of Thermoelectric-Erosion Based Turning Processes*

Dimensional accuracy, the surface quality of fabricated cylindrical components, and productivity of thermoelectric-erosion based turning processes largely depend on the appropriate selection of process parameters of thermoelectric-erosion-based turning processes. The smooth turning operation for a longer time at minimum tool wear and without wire

breakage (only for WTET) can be achieved by selecting appropriate process parameters of thermoelectric erosion-based turning processes. The process parameters of thermoelectric-erosion based turning processes are the same as normal thermoelectric-erosion based machining processes except for spindle rotational speed. The process parameters can be classified into two groups namely electrical parameters and non-electrical parameters as shown in Figure 3. The major electrical parameters are spark-on-time ( $S_{on}$ ), spark-off-time ( $S_{off}$ ), peak current ( $P_C$ ), servo-voltage ( $G_V$ ), and discharge energy (DE). Non-electrical parameters are dielectric/flushing pressure ( $W_P$ ), spindle rotational speed (SRS), types of dielectric, and electrode materials. Whereas, wire feed rate ( $W_{FR}$ ) and wire tension or wire rigidity ( $W_R$ ) are additional non-electrical parameters of the WTET process [21].

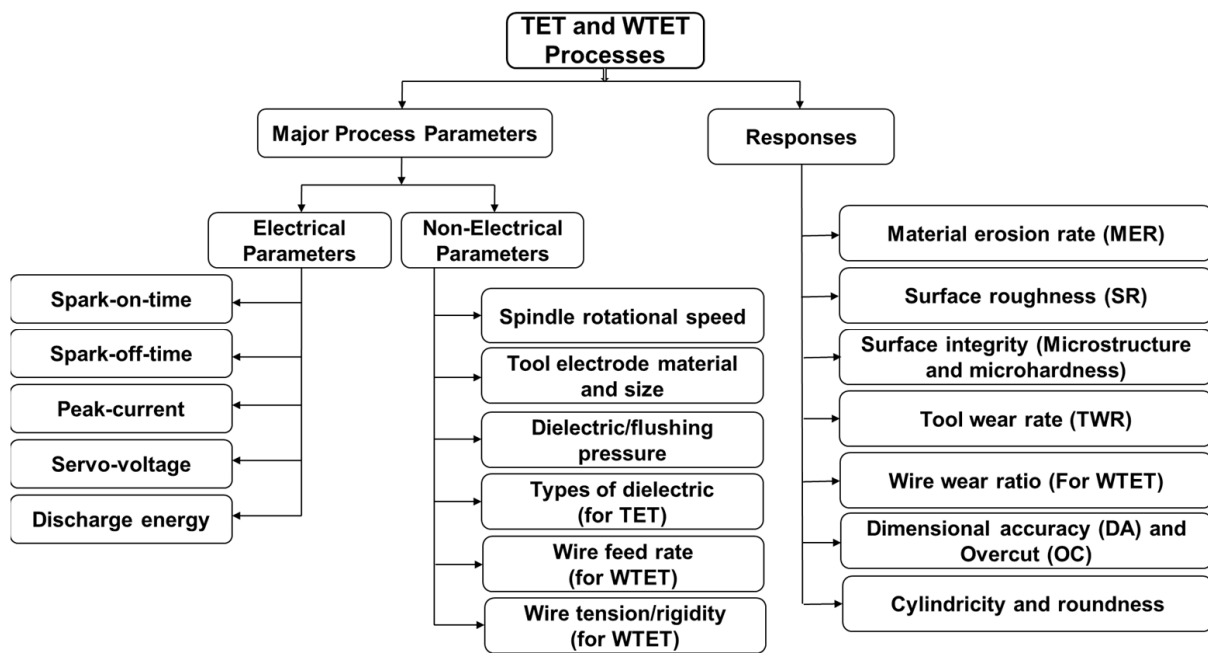


**Figure 3.** The process parameters and responses of thermoelectric-erosion based turning processes.

Spark-on-time ( $S_{on}$ ) indicates the time duration in microseconds during which sparks are generated between the inter-electrode gap (IEG). Spark-off-time ( $S_{off}$ ) represents the time duration in microseconds between happenings of two consecutive sparks. Material removal takes place during spark-on-time. Peak current ( $P_C$ ) is the extreme value of the current passing through the electrodes for the given pulse and its value is displayed directly on an ammeter equipped with a machine during the turning process. Servo voltage is the value of the voltage during the formation of the discharge channel between the IEG and the dielectric breaks down in the IEG. The discharge energy is the amount of heat released between the IEG. The discharge energy can be determined from the electrical parameters of TET and WTET. The higher values of the discharge energy result in a higher material erosion rate (MER). Flushing pressure ( $\text{kg}/\text{cm}^2$ ) is the pressure of the dielectric through IEG to flush away the eroded particles from there. Spindle rotational speed (SRS) is the rotational speed of the spindle per minute (RPM). The chuck or collet is attached to the spindle which holds the cylindrical workpiece. It is the most important parameter of TET and WTET processes and its higher values are desirable for straight and taper turning to achieve better surface quality and productivity. Wire feed rate is the rate at which the fresh wire continuously moves through the wire guides and the IEG for sparking. Its higher value is preferable for stable machining without wire breakage. Wire breakage increases the machining time and deteriorates the surface quality of the components and parts. Wire tension indicates the rigidity of wire between the wire guides. A high wire tension is desirable for stable machining and to avoid wire vibration. Wire vibration is responsible for short-circuiting and poor dimensional accuracy. Dielectric plays an important role in

thermoelectric-erosion based turning processes. It acts as a machining medium. EDM oil, kerosine, and hydrocarbons are used in TET whereas deionized water is used in WTET as a dielectric.

The aforesaid parameters significantly influence the performance measures such as erosion rate or material erosion rate (MER), surface roughness (SR), tool wear rate (TWR), wire wear ratio (WWR), surface quality, surface integrity, dimensional accuracy (DA), overcut (OC), cylindricity, and roundness. Therefore, the selection of optimal parametric conditions of TET and WTET is mandatory to fabricate better quality cylindrical parts with high productivity.

#### 1.4. Limitations of Thermoelectric-Erosion Based Turning Processes

Thermoelectric-erosion based processes have certain limitations such as (i) only suitable for electrically conducting materials; (ii) low material erosion rate than traditional machining processes, (iii) high capital cost; (iv) excessive tool electrode wear; (v) not suitable for mass production; (vi) requirements of fabricated tool electrodes in TET; and (v) flammable dielectrics (only TET process).

The next section presents a detailed review of the past work conducted on the fabrication of miniature cylindrical parts by various researchers using TET and WTET processes.

## 2. Review of Previous Research Work on Thermoelectric-Erosion Based Turning Processes

In the past decade, substantial research attempts have been reported on the fabrication of cylindrical and rotating parts from a variety of materials by contact and non-contact type turning operations. Non-contact or advanced machining methods and their variants such as TET, WTET, Strip-TET, and Hybrid-WTET were also used. In this paper, a critical review of the previous research is presented to (i) highlight the potential of the TET and WTET processes to fabricate better quality rotary parts and components; (ii) highlight the research findings of the previous work to recognize the scope and future directions of research in the same area. Tables A1 and A2 present a summary of the previous research work conducted on the fabrication of cylindrical and rotating parts by TET and WTET processes. The following sub-sections present their detailed discussion.

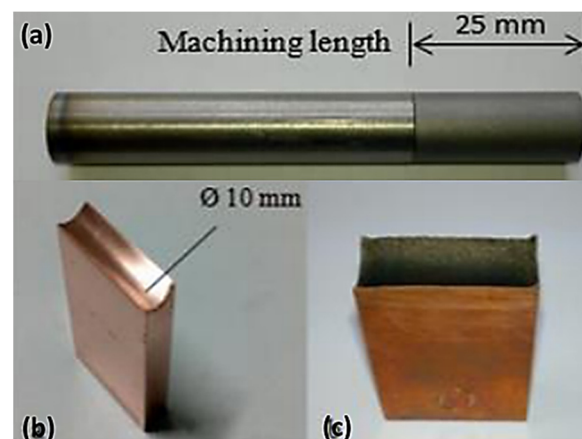
### 2.1. Review of Previous Research Work on Thermoelectric-Erosion Turning (TET)

Table A1 presents a summary of the previous work performed on thermoelectric-erosion turning (TET). Available literature indicates the little interest of researchers on TET to fabricate cylindrical parts in the last decades. The following sections present a detailed discussion of the previous work conducted on TET and its variants.

Sharp edge grooves were formed on an AISI D2 tool steel round bar (diameter: 20 mm; length: 200 mm) by an external magnetic-field assisted TET process using a 30 mm square copper electrode of 6 mm thick [22]. A total of nine experiments were designed and conducted according to Taguchi L<sub>9</sub> (4<sup>3</sup>) orthogonal array (OA) to identify the influence of magnetic flux density, pulse current, pulse duration, and spindle rotational speed on surface integrity (i.e., SR, recast layer thickness 'RLT', and hardness) of the turned surfaces. An optimum turning condition was obtained by grey relational analysis 'GRA' to minimize SR, RLT, and maximize hardness simultaneously. They found magnetic flux density and spindle rotational speed as the most influencing parameters on surface integrity as compared to other considered parameters. They also identified 0.4 T magnetic flux density, 5 A discharge current, 1000 μs spark-on-time, and 250 rpm spindle rotational speed as an optimal combination of turning parameters. An extensive review of the previous research on the fabrication of cylindrical parts and components from difficult-to-machine materials by thermoelectric-erosion based turning processes in the last decade was reported by [23]. They highlighted the different methods of thermoelectric-erosion based turning processes (i.e., strip-TEM, sinker-TEM, WTET, and hybrid WTET) using an external belt-driven rotary

attachment having a chuck or collet to hold the workpiece. The future research directions were also highlighted to encourage further work in the same area.

Gohil and Puri [24,25] worked extensively on thermoelectric- erosion turning (TET). They successfully performed straight turning on a solid cylindrical-shaped bar made of titanium alloy Ti-6Al-4V (diameter: 10 mm; Length: 75 mm) by TET using a rectangular strip of copper having dimensions of 40 mm × 25 mm × 8 mm as a tool electrode (Figure 4). A total of 18 experiments were designed and conducted according to Taguchi's  $L_{18}$  ( $2^1 \times 3^7$ ) OA to identify the effects of TET process parameters such as peak current, spark-on-time, gap voltage, spindle rotational speed, and tool thickness on MER, SR, and TWR during straight turning of titanium bar. The turning operation was carried out for 25 min in each experiment. After conducting an analysis of variance and optimization, they concluded that (i) better surface finish can be achieved by TET using a rectangular copper electrode; (ii) better MER and lower SR can be achieved at 5  $\mu$ s spark-on-time, 5 A peak current, 40 V gap voltage, 40 rpm spindle rotational speed; (iii) peak current, gap-voltage, and spark-on-time significantly affect MER; and (iv) peak current and spark-on-time have a significant influence on SR.



**Figure 4.** TET turned titanium bar and rectangular copper tool electrode: (a) turned titanium bar; (b) copper tool electrode before turning; (c) copper tool electrode after turning (Reprinted/Adapted with permission from [25]. 2018, Elsevier. ©).

Gohil and Puri [26] successfully performed straight turning on stainless steel (SS 304) bar having 10 mm diameter and 75 mm long by TET using a preshaped rectangular solid copper electrode having dimensions of 40 mm long, 25 mm wide, and 8 mm thick. A total of 36 experiments were planned and conducted according to the full factorial design (FFD) approach of Design of Experiments (DoE) by assigning  $S_{on}$  and IP with three levels, and voltage and tool thickness with two levels. Each experiment was performed for 15 min on a 25 mm length of SS 304 bar at a constant spindle speed of 50 rpm and flushing pressure of 0.05 kg/cm<sup>2</sup>. They identified spark-on-time ( $S_{on}$ ) as the most significant parameter that effectively influences the MER and TWR. They also found that interaction between  $S_{on}$  and IP has more influence on MER and TWR. Jadidi et al. [27] fabricated sharp edge grooves on an AISI D2 tool steel round bar (diameter: 10 mm; length: 75 mm) by an external magnetic-field assisted TET process using a copper electrode with a 30 mm squared face and 8 mm thickness. The spindle rotation speed was varied through a belt and pulley driving system. FFD-based 81 experiments were conducted by varying the pulse current, pulse duration, spindle rotational speed, and magnetic flux density at three levels each. Each experiment was conducted for 120 min to identify the effects of selected variable parameters on MER and OC. They found that (i) magnetic field is more significant compared to other variable parameters; (ii) application of magnetic field improves 42% MER as compared to traditional TET, and (iii) spindle rotational speed enhanced dimensional accuracy up to 23% but has a negligible effect on MER.

Matoorian et al. [28] used TET having a rotary spindle attached with a collet (Figure 5) for making 8 mm wide grooves on a 6 mm diameter cylindrical bar made of high-speed steel, by a copper block having dimensions of 50 mm × 10 mm × 8 mm. Experiments were planned and conducted according to Taguchi  $L_{18}$  ( $2^1 \times 3^7$ ) orthogonal array (OA) and each experiment was repeated thrice. Thus, a total of 54 experiments were conducted by considering 25 min as the total machining time for each experiment to identify the effect of peak current, spark-on-time, voltage, spark-off-time, servo, and spindle rotational speed on MER. Signal-to-noise (S/N) ratios were used for optimization and a mathematical model was developed by regression analysis to predict MER. They reported that (i) intensity, spindle rotational speed, servo voltage, and spark-on-time as significant parameters for MER; and (ii) 6 A peak current, 50  $\mu$ s spark-on-time, 20  $\mu$ s spark-off-time, 120 V voltage, 30 V servo voltage, and 40 rpm spindle rotational speed as optimum turning combination to improve the productivity.

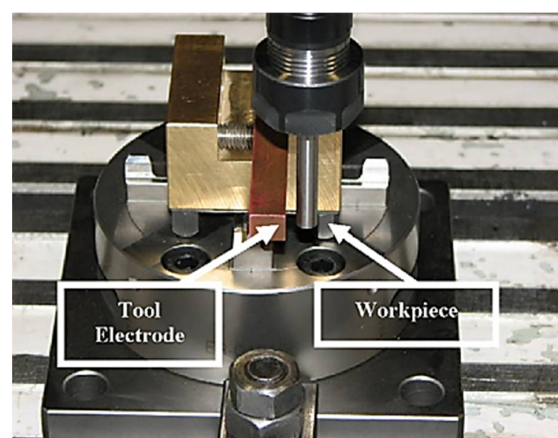


Figure 5. Experimental setup (Reprinted/Adapted with permission from [28]. 2008, Elsevier.©).

Rehman et al. [29] fabricated 8 mm wide and 20 mm deep groove on cylindrical AISI D2 tool steel ( $\phi$ : 10 mm; L: 200 mm) by TET using a 30 mm square copper block with 6 mm thickness. The discharge current and spark-on-time were identified as the most influencing parameters for MER and hardness. The optimum parameters for finish turning are 0.4 T magnetic flux density, 5.3 A discharge current, 600  $\mu$ s Spark-on-time, and 250 rpm spindle rotational speed. A new method was developed for turning cylindrical bar known as strip-TET as shown in Figure 6. An axial-symmetric shape (Figure 7) was formed on a 3 mm diameter and 200-long cylindrical bar made of SS 304 stainless steel in multiple turning stages (i.e., six-stage) by TET using 0.1 mm thick and 10 mm wide brass strip as tool electrode at constant spindle rotational speed. Higher MER can be achieved by strip-TET compared to WTET.

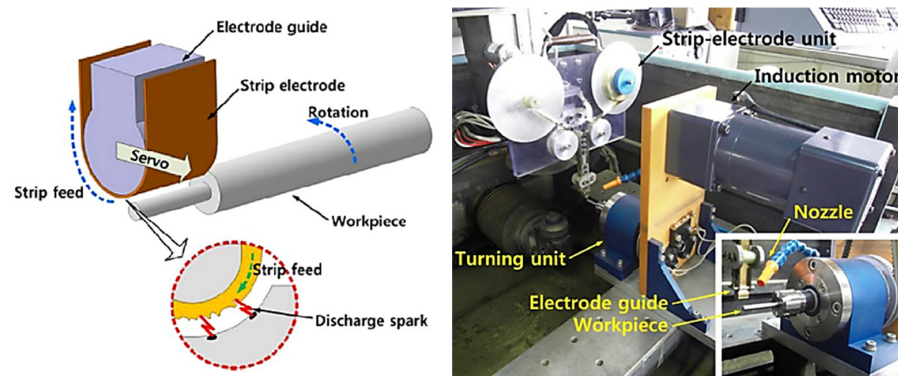
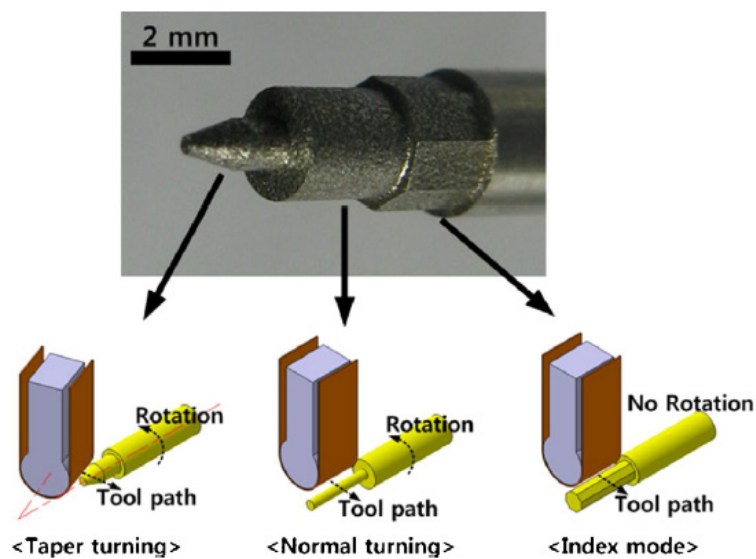


Figure 6. Schematic diagram of Strip-TET along with Strip-TET setup (Reprinted/Adapted with permission from [30]. 2013, Elsevier. ©).



**Figure 7.** An axial-symmetric shape fabricated by Strip-TET process (Reprinted/Adapted with permission from [30]. 2013, Elsevier. ©).

## 2.2. Review of Previous Research Work on Wire-Assisted Thermoelectric-Erosion Turning (WTET)

Table A2 presents a summary of the previous work performed on wire-assisted thermoelectric-erosion turning. Available literature indicates the considerable interest of researchers on WTET to fabricate cylindrical parts in the last decades. The following sections present a detailed discussion of the previous work conducted on WTET and its variants.

Bergs et al. [31] fabricated testing shafts made of case-hardened steel (18CrNiMo7-6) with better dimensional accuracy and varying surface qualities by the WTET process with the help of an indexing rotary single-axis table and 250  $\mu\text{m}$  diameter of brass wire. An analogy disk-on-disk test rig was used and the fatigue strength of the WTET fabricated shafts was found sufficient for the required application. Oswal et al. [32] performed turning on Ti-6Al-4V (grade 5) cylindrical bar using the WTET process. They identified 75 rpm SRS, 10  $\mu\text{s}$   $S_{\text{on}}$ , and 14 m/s as  $W_{\text{FR}}$  as the optimum parameter combination. They observed a 16% improvement in the surface quality and a 1% improvement in MER after machining at an optimized setting. Srivastava et al. [33] performed a turning operation on a newly developed cylindrical bar made from a hybrid metal matrix composite of aluminum (A359/B4C/ $\text{Al}_2\text{O}_3$ ). The major objective of this work was to study the effect of spindle rotational speed on the surface integrity namely surface roughness, the morphology of the recast layers, microhardness, and residual stresses of the turned bar. They observed several peaks and valleys with small-scale defects such as surface porosity on the turned surface. They concluded that a better surface finish can be achieved at high spindle rotational speed.

In an important study, the micro-rotating parts were fabricated from the cylindrical bars made of Cemented carbide (K15) by WTET process in multi-steps (i.e., rough turning 'RT', semi-finished turning 'SFT', and finished turning 'FT') using tungsten wire of 30  $\mu\text{m}$  diameter and TEM oil as the dielectric [34]. They successfully fabricated micro balloons probe of 98.7  $\mu\text{m}$  diameter having 0.435  $R_a$  by WTET using a newly developed rotary setup.

Gjeldum et al. [35] experimentally investigated the effect of variable parameters such as peak-current, spark-on-time, and spindle rotational speed on material erosion rate, during the turning of a 4.75 mm diameter cylindrical bar made of X5CrNi18-10 steel material. They performed straight turning to fabricate 1.5 mm of a cylindrical bar with a 6 mm length of cut at 1.65 mm depth of cut. Giridharan and Samuel [36] performed turning of 10 mm diameter AISI 4340 steel round bar having a length of 75 mm by WTET process using brass wire of 250  $\mu\text{m}$  diameter in the presence of continuous flowing deionized water having conductivity 200 mS [36]. They concluded that (i) surface crack

developed at higher discharge energy; (ii) RLT increases with the increase in discharge energy; (iii) 3-D surface topography revealed the turbulent nature of the turning process due to transient erosion by WTET; (iv) higher MER (0.06 g/min) with an average roughness of 4.5–5.5  $\mu\text{m}$  can be achieved at 1.6–2.6 J consumption of discharge energy. A computational technique was proposed by George et al. [19,37] to develop the model for crater formation during the turning of a 10 mm diameter round bar made of Inconel 825 by WTET using 250  $\mu\text{m}$  diameter of brass wire. Hosseini et al. [38] performed twenty-seven experimental runs based on  $L_{27}$  Taguchi's ( $3^3$ ) OA to investigate the effects of WTET parameters such as discharge current, spark-on-time, and SRS on fatigue life, SR, residual stress, and hardness. Each experiment was performed on a 112 mm long and 12 mm diameter cylindrical bar made of Inconel 718 by WTET process using 250  $\mu\text{m}$  diameter brass wire and deionized water as a dielectric. The outcomes revealed that the maximum fatigue life of about 14,400 cycles can be achieved at optimum turning conditions (i.e., 5 A discharge current, 600  $\mu\text{s}$   $S_{\text{on}}$ , and 250 rpm SRS). They identified  $P_C$ , SRS, and  $S_{\text{on}}$ , as the most significant parameters. They also found that SR is mainly influenced by SRS while residual stress is influenced by discharge current.

An important study reports the effect of power, spark-off-time, voltage, and SRS on MER, SR, and roundness during straight turning of the cylindrical bar of AISI D3 tool steel by WTET using 250  $\mu\text{m}$  diameter brass wire and flushing deionized water [39,40]. Figure 8 shows the WTET with the rotary setup used for turning in this study. They identified higher values of power and voltage, and lower values of  $S_{\text{off}}$  and SRS to improve productivity.

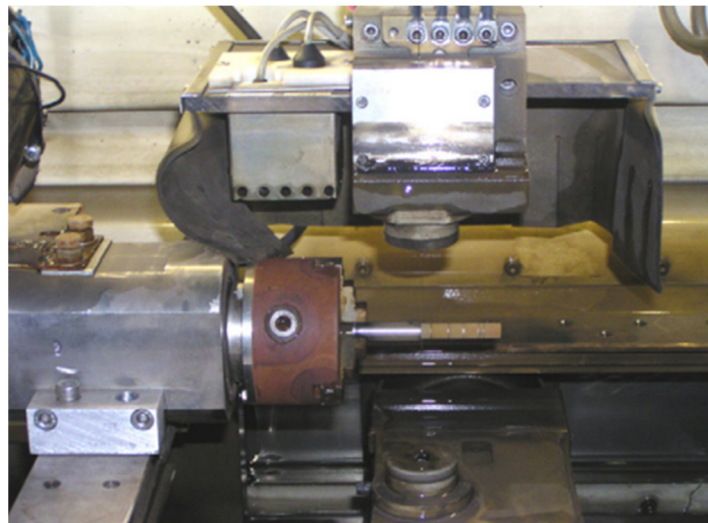


**Figure 8.** WTET with rotary setup (Reprinted/Adapted with permission from [39]. 2008, Elsevier. ©).

A group of researchers developed a rotary setup and conducted the turning of a cylindrical brass rod of 9.45 mm diameter by WTET using 250  $\mu\text{m}$  diameter brass wire [41]. Their investigation results can be summarized as (i) SR and MER were significantly influenced by feed rate and radial DOC, respectively; (ii) the developed models were significant for selected responses with prediction error less than 7%; and (iii) 4.525  $\mu\text{m}$  SR and 19.147  $\text{mm}^3/\text{min}$  MER can be achieved by using optimized parameters. An interesting study reports the effectiveness of NSGA-II for a successful optimization in WTET to secure the best erosion rate and surface finish of 10 mm diameter cylindrical AISI D3 steel rod [42]. Mondal and Bose [43] fabricated micro-pins from 2 mm diameter and 25 mm long cylindrical bars made of electrolytic-tough-pitch copper (ETP Cu) by WTET process using 250  $\mu\text{m}$  diameter brass wire and deionized water to remove the eroded particles from IEG. Figure 9 shows the WTET fabricated high-aspect-ratio micro-pins. They fabricated 15 mm long cylindrical pins of 500  $\mu\text{m}$  diameter by WTET process in each experiment. They identified spark-on-time as the most influencing parameter for dimensional inaccuracy compared to other selected

parameters. They also reported that minimum dimensional inaccuracy of 0.455 mm can be achieved at  $38 \mu\text{s } S_{\text{off}}$ ,  $9 \mu\text{s } S_{\text{on}}$ , 1142 rpm SRS, and 72 V servo voltage.



**Figure 9.** WTET fabricated high-aspect-ratio micro-pins (Reprinted/Adapted with permission from [43]. 2020, Elsevier. ©).

A new technique was proposed by Mohammadi et al. [44] to perform turning on difficult-to-machine materials by WTET using brass wire of 250  $\mu\text{m}$  diameter and deionized water. In this technique, ultrasonic vibration was introduced to the brass wire to improve the productivity of WTET. A total of 36 experiments were conducted to perform the turning operation (6.5 mm turning length and 0.6 depth of cut) on a 10 mm diameter cylindrical bar made of cemented steel by WTET in each experiment. They investigated the effects of ultrasonic vibration, discharge power, spark-off-time, and SRS on MER. They concluded that (i) productivity (i.e., MER) can be improved by applying ultrasonic vibration; (ii) ultrasonic vibration has the most influence on MER in finishing and roughing turning; and (iii) MER up to  $2.08 \text{ mm}^3/\text{min}$  can be achieved at optimum turning condition of 10 A power,  $4 \mu\text{s } S_{\text{off}}$ , 45 rpm SRS. Mohammadi et al. [45] performed straight turning on 10 mm diameter of cemented steel cylindrical bars by WTET using 250  $\mu\text{m}$  diameter brass wire and localized flushing deionized water. Figure 10 shows the rotary setup with an ultrasonic head in a five-axis WTET machine. Twenty-seven experiments were performed by turning on a 10 mm length of the cylindrical bar with a 2 mm depth of cut in each experiment. They concluded that (i) power, voltage, and servo voltage are important factors that influence productivity (MER); and (ii) SRS and wire rigidity have the least influence on MER.

Naik et al. [46–50] conducted a study where they performed the turning operation on a 50 mm long cylindrical bar having 10 mm diameter made of Inconel 718 by WTET process using 250  $\mu\text{m}$  diameter of zinc-coated brass wire in the presence of deionized water. The eighteen experimental runs were conducted to identify the influence of processes parameters such as SRS, spark-on-time, spark-off-time, servo voltage, feed rate of wire; dielectric pressure on MER and SR. They reported that (i) N 250 rpm,  $124 \mu\text{s } S_{\text{on}}$ ,  $40 \mu\text{s } S_{\text{off}}$ , 18V  $G_V$ , 2 m/min  $W_{\text{FR}}$ , 1.8 bar  $W_P$  as optimum turning conditions; (ii)  $S_{\text{on}}$  has the most significant influence on MER and SR [48]; (iii) 3.59% improvement in MER and 9.17% decrement in SR; (iii) MER increases with increase  $S_{\text{on}}$  and SRS and decreases with the increase of servo voltage and  $W_{\text{FR}}$  to a certain level; and (iv) 9.5% improvement in MER and 43.17% reduction in SR by results obtained from ANOM based confirmation test [50].

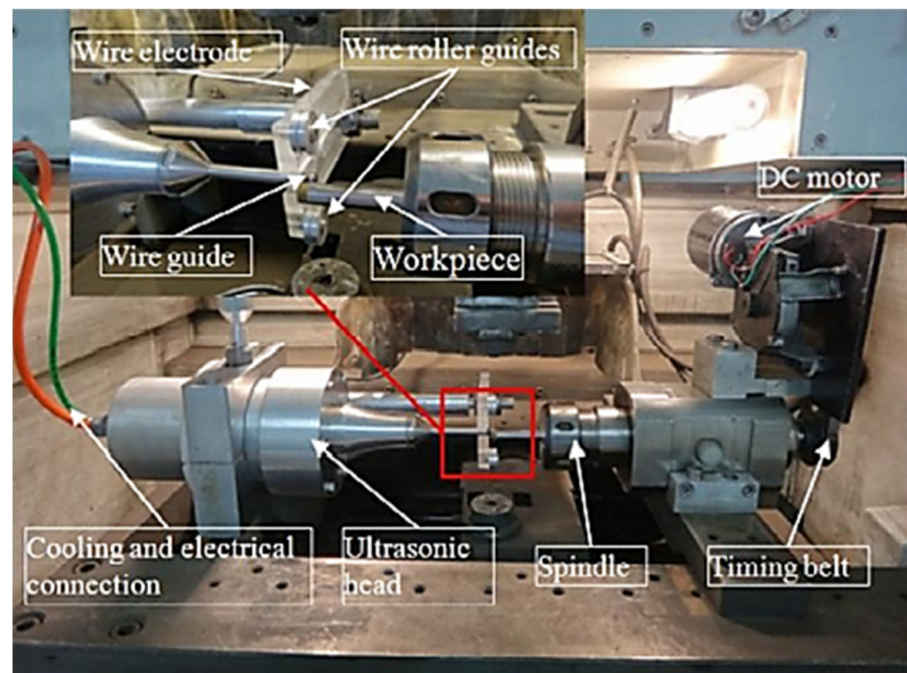


**Figure 10.** Rotary setup with ultrasonic head in five-axis WTET machine (Reprinted/Adapted with permission from [44]. 2013, Elsevier. ©).

The effects of WTET input parameters namely SRS, spark-on-time, spark-off time, servo-voltage, wire feed rate, and dielectric flow rate on SR during turning (turning length: 50 mm) of Inconel 718 cylindrical bar (diameter: 10 mm; length: 50 mm) using 250  $\mu\text{m}$  diameter of zinc-coated brass wire, were investigated [51]. It was found that (i)  $S_{\text{on}}$  has the most significant influence on SR; (ii) SR decreased with an increase in  $S_{\text{off}}$ , servo voltage, and  $W_{\text{FR}}$ ; (iii) prediction error obtained from the developed model is less than 8% and validated experimentally. Nag et al. [52] investigated the influence of variable parameters namely spark-on-time, spark-off-time, gap-voltage, and SRS on considered responses such as MER, SR, and WWR during straight turning of 30 mm long and 8.0 mm diameter of cylindrical BAR OF titanium (Ti6Al4V) by WTET process using 250  $\mu\text{m}$  diameter of Zn-coated brass wire and deionized water. A total of 31 experiments based on CCD of RSM were conducted to perform 1.5 mm deep and 3 mm long turning on cylindrical titanium bar in each experiment. ANOVA, regression models, and DFA were applied to find out significant parameters, predict the responses, and obtain optimum turning conditions, respectively. They concluded that (i) MER, SR, and WWR decrease with an increase in  $S_{\text{off}}$ , gap-voltage, and SRS; (ii) SR (1.99  $\mu\text{m}$  – 1.37  $\mu\text{m}$ ), MER (7.55–13.66  $\text{mm}^3/\text{min}$ ), and WWR (0.05–0.08) can be achieved by WTET; and (iii) 1.131  $\mu\text{m}$  SR, 17.33  $\text{mm}^3/\text{min}$  MER and 0.0346 WWR can be achieved using optimal turning combination.

Patel and Patel [53] developed a cylindrical holding device using a motor and belt-driven drilling chuck to perform the turning operation of a GCr15 Bearing steel bar of 4.75 mm diameter by WTEM using 250  $\mu\text{m}$  diameter of brass wire.  $P_C$  was found as the most valuable factor for MER and SR. They reported that maximum MER (4.2  $\text{mm}^3/\text{min}$ ) can be achieved at 90  $\mu\text{m}$  rotational infeed. In a comparative study, researchers found rotary-WTET superior to wire-assisted TEM for material erosion rate [54]. Roy and Mandal [55] proposed a multi-stage WTET process to fabricate the cylindrical surface with better surface characteristics at high productivity. Taper turning of 8 mm diameter and 100 mm long cylindrical bar made of Nitinol 60 was performed by WTET process using 250  $\mu\text{m}$  diameter of Zn-coated brass wire and deionized water. Higher volumetric-MER (i.e. VMER) and lower values of  $R_a$  can be achieved at higher values of SRS and inclination angle 'IA', and both parameters were found as the most influential for cracks and craters formation on the WTET turned surfaces.

A new concept was proposed for turning operation known as low-speed wire-assisted thermoelectric-erosion turning (LS-WTET) to fabricate micro-rods made from cylindrical bars made of carbon steel (ASTM 1045) and titanium alloy (TC4) in multiple-turning stages namely RT, SFT, and FT using brass wire of 250  $\mu\text{m}$  diameter [56–58]. LS-WTET was also used to fabricate spiral grooves (width: 1.5 mm and depth: 0.4 mm), micro rods, and two edge cutting tools from tungsten Carbide (YG8) cylindrical bar ( $\phi$ : 3 mm; L: 40 mm). Their comprehensive investigation concluded that (i) 1000  $\mu\text{m}$  long and 70  $\mu\text{m}$  diameter micro-rod with better surface quality and dimensional accuracy can be manufactured by LS-WTET; (ii) very shallow and elliptical-shaped craters were formed on TC4 micro bar fabricated by LS-WTET; (iii) cracks formation were invisible in FTT; (iv) surface and sub-surface damages in LS-WTET turned microbars can be minimized effectively in the multiple turning stages; and (v) a taper pin of 40  $\mu\text{m}$  diameter and a micro-turning can be manufactured by LS-WTET; (v) SRS and feed speed have a significant effect on the error in roundness; and (vi) groove width decreases with the increase of wire rigidity and feed speed.

Another investigation reveals the successful fabrication of spirals microelectrode and spirals micro-cutting tools from a 2.8 mm diameter of YG8 cylindrical rod by LS-WTET using 200  $\mu\text{m}$  diameter of brass wire and deionized water (5  $\mu\text{S}/\text{cm}$ ) [59]. These microelectrodes and spiral micro-cutting tools/electrodes (as shown in Figure 11) were fabricated in multiple turning stages (i.e., RT, SFT, FT) by WTET. The average diameter and length of the fabricated micro-cutting tool are 175.77  $\mu\text{m}$  and 1300  $\mu\text{m}$ , respectively. This study explored the potential of the WTET process to fabricate complex cylindrical structures from difficult-to-machine materials. Talebizadehsardari et al. [60] conducted WTET of Inconel 718 for making cylindrical bars. The material erosion rate was maximized at 15 A discharge current, 800  $\mu\text{s}$   $S_{\text{on}}$ , and 250 SRS. A comprehensive review of the previous work on WTET of difficult-to-machine materials was reported [61]. The influence of WTET process parameters on considered responses namely MER, SR, roundness, RLT, and crater formation was reported in this review paper. They also highlighted the future research directions of the WTET process to motivate the researchers working in the same area.

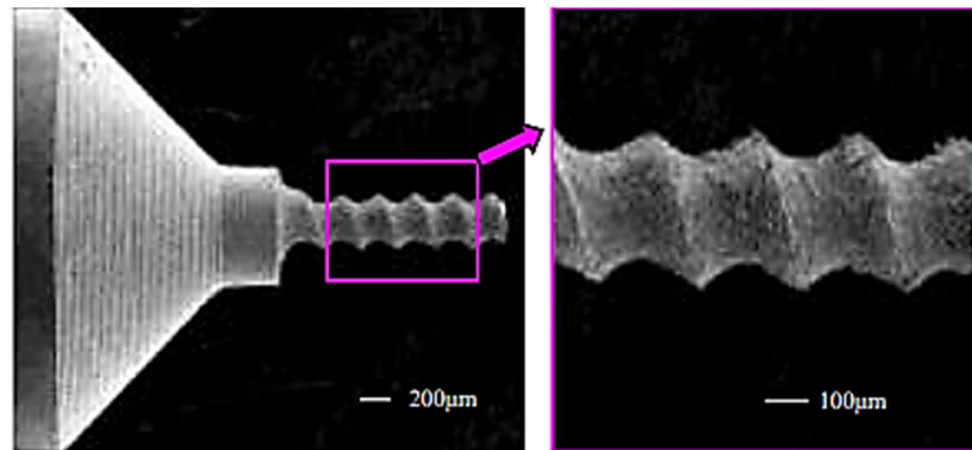


**Figure 11.** SEM images of spirals microelectrode fabricated by LS-WTET process (Reprinted/Adapted with permission from [59]. 2018, Elsevier. ©).

Vignesh and Ramanujam [62] successfully performed straight turning on titanium alloy (Grade 5) round bar of 10 mm diameter by WTET process using 250  $\mu\text{m}$  diameter brass wire and deionized water (having conductivity 5  $\mu\text{S}/\text{cm}$ ) as the dielectric. They found increasing MER with higher values of  $S_{\text{on}}$ ,  $W_{\text{FR}}$ , and SRS; and decreasing surface roughness with higher values of  $W_{\text{FR}}$ , and SRS. A new turning setup was successfully used in [63] to form the micro-grooves on a rotating cylindrical bar made of K15 and Z100CD17 bearing steel materials by WTET using 30  $\mu\text{m}$  diameter of tungsten wire and deionized water acts as the dielectric. Wang et al. [64] used LS-WTET to fabricate micro-grooves

on a cylindrical bar made of Gcr15 bearing steel having 20 mm internal diameter, 28 mm external diameter, and 28 mm length. The zinc-coated brass wire of 250  $\mu\text{m}$  diameter and deionized water were used as tool electrodes and dielectric, respectively. The experimental runs were carried out to identify the influence of the spindle rotational speed, wire feed rate, wire feed rate, and wire rigidity on roundness, SR, and surface morphology during the 23  $\mu\text{m}$  deep and 25  $\mu\text{m}$  long turning of the Gcr15 cylindrical bar. They successfully fabricated microgrooves by the LS-WTET process. It was found that wire tension with smaller axial vibration can significantly improve roundness and reduce surface roughness, and lower values of wire feed rate significantly increase the surface roughness.

Zhu et al. [62–66] successfully fabricated high aspect ratio micro-bars of 40  $\mu\text{m}$  diameter from a cylindrical bar of 3.9 mm diameter made of GCr15 steel by WTET process using 200  $\mu\text{m}$  brass wire and deionized water as tool electrode and dielectric, respectively. Figure 12 depicts the micro-parts fabricated by them using the WTET process. They successfully fabricated a set of high-aspect-ratio pin-electrodes having 40  $\mu\text{m}$  as the minimum diameter and 60 as the aspect ratio by the WTET process. They made successful attempts to maximize the material erosion rate and minimize surface roughness.

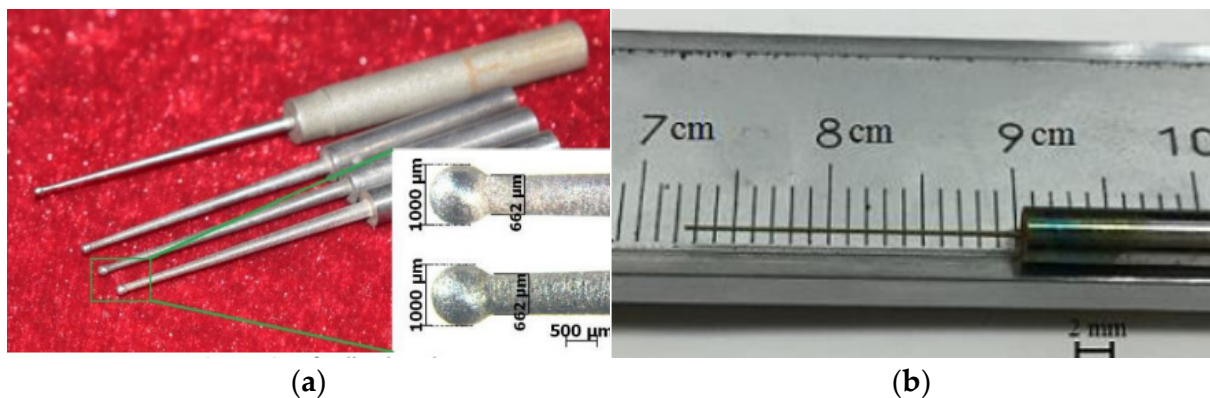


**Figure 12.** Cylindrical micro-parts fabricated by WTET process: (a) micro-bars; and (b) micro-pins (Reprinted/Adapted with permission from [65]. 2016, Elsevier. ©).

The straight turning was performed on Ti-6Al-4V titanium alloy cylindrical bars having 9.49 mm diameter and 20 mm in length by WTET process using 250  $\mu\text{m}$  diameter of brass wire and deionized water acts as the dielectric. The influence of pulse intensity, voltage, wire rigidity, and SRS on surface roughness was investigated during the turning of micro-cylindrical components [67]. It was reported that (i) WTET has the potential to fabricate cylindrical micro-parts made of titanium by WTET process; (ii) lower values of pulse intensity and voltage can significantly decrease the surface roughness; (iii) 4.0143  $\mu\text{m}$  and 5.9% as surface roughness and relative error, respectively; (iv) violent sparks are generated at higher values of pulse intensity and voltage results in the formation of wide and deep craters on turned surfaces of cylindrical micro-parts lead to rough surfaces.

From the critical review of the previous work, it can be said that WTET has more potential than the TET process to fabricate high-precision cylindrical parts. The major drawback of the TET process is the requirement of different fabricated strip-electrodes to manufacture a variety of cylindrical parts. Whereas, there is as such no requirement in the WTET process in which a fine wire is used for fabricating all kinds of cylindrical parts. The setup time in the TET process is more as compared to WTET. The better dimensional accuracy and surface quality of cylindrical parts can be achieved by WTET than the TET process. But wire breakage is a major issue in the WTET process which affects productivity. Strip-electrodes can be reused but wire cannot be reused for the turning process. There are some limitations and benefits to both of the processes.

### 3. Conclusions

This review paper presented a detailed overview of the previous work on turning cylindrical bars to make miniature size parts by thermoelectric-erosion based turning processes (i.e., TET and WTET). The following conclusions can be drawn:

- [i] Previous work revealed that almost researchers used a belt-driven rotary spindle attached with a chuck or collet to hold the cylindrical workpiece firmly at a rotating speed to perform turning operation by WTEM processes.
- [ii] Most of the previous work is performed on turning the solid circular bars only.
- [iii] Most of the work has been performed on turning the circular bar by WTET and very little work has been performed on turning by the TET process.
- [iv] Higher MER and non-breaking rectangular electrodes are major advantages of the TET process.
- [v] TET has the potential to produce groove and turning operation on long machining length without breakage of tool electrode.
- [vi] WTET can produce good quality miniature parts on cylindrical bars from difficult-to-machine materials.
- [vii] The past research is mostly limited to the investigation of the material erosion rate and surface roughness during turning by TET and WTET.
- [viii] Limited work has been conducted on modeling and optimization of TET and WTET process parameters for enhancement in quality, productivity, and sustainability.

### 4. Future Research Directions

The following future research directions are identified from the review of past work:

- [i] Development of a rotary table that should have a varying range of rotational speed facilitating TET and WTET of cylindrical parts.
- [ii] Investigations on energy consumption and consumption of consumables by TET and WTET processes.
- [iii] Exploring TET and WTET to perform micro to meso-sized taper turning on difficult-to-machine-materials.
- [iv] Investigating stepped turning on difficult-to-machine materials by TET and WTET.
- [v] Exploring the effect of assistance of magnetic field and vibrations on the performance of the WTET process during turning.
- [vi] Improving productivity and sustainability of the TET and WTET process by optimization and life cycle analysis.

**Author Contributions:** Conceptualization, methodology, organizing, writing—original draft, S.K.C.; supervision, writing—review and editing, K.G. All authors have read and agreed to the published version of the manuscript.

**Funding:** This research received no external funding, and the APC is funded by [University of Johannesburg].

**Data Availability Statement:** The study did not report any data.

**Conflicts of Interest:** The authors declare that they have no conflict of interest.

### Nomenclature

TET	Thermoelectric-erosion turning
WTET	Wire-assisted thermoelectric-erosion turning
$S_{on}$	Spark-on-time
$S_{off}$	Spark-off-time
$P_c$	Peak-current
$G_V$	Servo-voltage
DE	Discharge energy

---

$W_{FR}$	Wire feed rate
$W_R$	Wire rigidity
$W_P$	Flushing pressure
SRS	Spindle rotational speed
MER	Material erosion rate
SR	Surface roughness
TER	Tool erosion rate
WWR	Wire wear ratio
SQ	Surface quality
SI	Surface integrity
DA	Dimensional accuracy
OC	Overcut
RL	Recast layer
RLT	Recast layer thickness
SEM	Scanning electron microscope
XRD	X-ray Powder Diffraction
DoE	Design of Experiments
DTM	Difficult-to-machine
HAR	High-aspect-ratio
OA	Orthogonal array
CCD	Central composite design
RSM	Response surface methodology
ANOVA	Analysis of variance
FFD	Full factorial design
GRA	Grey relational analysis
RA	Regression analysis
DFA	Desirability function analysis
S/N	Signal-to-noise
DOC	Depth of cut
TD	Turning diameter
TL	Turning length

## Appendix A

**Table A1.** Summary of the previous work on the fabrication of cylindrical and rotating parts by TET process.

Researchers (Year) [Ref. no.]	Turning Specifications	Workpiece, Tool Electrode, and Dielectric	Process Parameters	Responses	Key Findings/Remarks
Azhiri et al. (2020) [22]	Meso-sized turning Type: Grooves	AISI D2 round bar ( $\phi$ : 20 mm; L: 200 mm); Electrode: copper (L30 $\times$ W30 $\times$ T6 in mm)	Magnetic flux density, $P_C$ , Pulse duration, and SRS	RLT, SR, and Micro-hardness	<ul style="list-style-type: none"> <li>Found magnetic flux density and SRS as the most influencing parameters on surface integrity as compared to other considered parameters.</li> <li>Observed work rotational speed as the most significant parameter with a noteworthy effect on considered responses.</li> </ul>
Gohil and Puri (2015) [23]	-	-	-	-	<ul style="list-style-type: none"> <li>Reported the previous research work conducted on turning by thermoelectric-erosion based processes.</li> </ul>
Gohil and Puri (2016) [24]	Meso-sized turning (M/C Time: 25 min) ( $\phi$ : 10 mm; TL: 25 mm) Type: Straight turning	Titanium Ti-6Al-4V alloy ( $\phi$ : 10 mm; L: 75 mm); Electrode: copper (8mm $\times$ 25mm $\times$ 40mm and 5 mm radius); Dielectric: EDM oil	$P_C$ , $S_{on}$ , $G_V$ , SRS, and $W_P$	MER and SR	<ul style="list-style-type: none"> <li>Validated error less than 6%.</li> <li>Identified peak current, gap voltage, and spark-on time as the most significant parameters for MER.</li> <li>Identified peak current and spark-on time as the most significant parameters for SR.</li> </ul>
Gohil and Puri (2018) [25]	Meso-sized turning (M/C Time: 25 min) (TL: 25 mm) Type: Straight turning	Titanium Ti-6Al-4V alloy ( $\phi$ : 10 mm; L: 75 mm); Electrode: copper (L40 $\times$ W25 $\times$ T8 in mm)	$P_C$ , $S_{on}$ , $G_V$ , SRS, and $W_P$	MER and SR	<ul style="list-style-type: none"> <li>Successfully performed turning of titanium bar by TET process using a rectangular copper electrode.</li> <li>Identified 5 <math>\mu</math>s <math>S_{on}</math>, 5 A <math>P_C</math>, 40V <math>G_V</math>, 40 rpm SRS and 0 kg/cm<sup>2</sup> WF as optimal turning conditions using Taguchi-based GRA.</li> </ul>
Gohil and Puri (2018) [26]	Meso-sized turning (M/C Time: 15 min) ( $\phi$ : 10 mm; TL: 25 mm) Type: Straight turning	SS-304 stainless steel ( $\phi$ : 10 mm; L: 75 mm); Electrode: copper (L40 $\times$ W25 $\times$ T8 in mm); Dielectric: EDM oil	$S_{on}$ , $P_C$ , $G_V$ , and tool thickness	MER and TWR	<ul style="list-style-type: none"> <li>Identified <math>S_{on}</math> as the most significant parameter that effectively influences the MER and TWR.</li> <li>Also identified voltage and tool thickness as significant parameters after pulse on time.</li> </ul>

Table A1. Cont.

Researchers (Year) [Ref. no.]	Turning Specifications	Workpiece, Tool Electrode, and Dielectric	Process Parameters	Responses	Key Findings/Remarks
Jadidi et al. (2020) [27]	Meso-sized turning (M/C Time: 120 min) Type: Groove	AISI D2 round bar ( $\phi$ : 20 mm; L: 200 mm); Coppe electrode: (L30 $\times$ W30 $\times$ T6 in mm)	Magnetic flux density, Pulse current, Pulse duration, SRS	MER and OC	<ul style="list-style-type: none"> <li>Identified magnetic field as the most significant parameter.</li> <li>Achieved higher MER and better dimensional accuracy at a high-intensity magnetic field (i.e., 0.4 T).</li> </ul>
Matoorian et al. (2008) [28]	Meso-sized turning (M/C Time: 30 min) (Width: 6 mm; TL: 8 mm) Type: Straight turning	High-speed steel ( $\phi$ : 6 mm; L: mm); Pure copper electrode (L8 $\times$ W10 $\times$ T50 in mm)	$P_c$ , $S_{on}$ , $S_{off}$ , Voltage, Servo, and SRS	MER	<ul style="list-style-type: none"> <li>Identified intensity, SRS, servo, and spark-on time as the most significant parameters.</li> <li>Developed a mathematical model to predict MER.</li> <li>Identified optimum setting to maximize productivity.</li> </ul>
Rehman et al. (2021) [29]	Meso-sized turning (Width: 6 mm; TL: 6 mm; Depth: 20 mm) Type: Grooves	AISI D2 ( $\phi$ : 10 mm; L: 200 mm); Copper eelectrode: (L30 $\times$ W30 $\times$ T6 in mm)	Magnetic flux density, Current, $S_{on}$ , and SRS	MER, OC, SR, RLT, and Hardness	<ul style="list-style-type: none"> <li>Observed discharge current and spark-on-time, and spark-off-time as the most significant parameter for MER and hardness.</li> <li>Identified magnetic flux density as the most significant parameter for OC, Ra, and RLT.</li> </ul>
Song et al. (2013) [30]	Meso-sized turning (M/C Time: 25 min) (DOC: 0.1 mm) Type: Straight turning	Stainless steel 304 ( $\phi$ : 3.0 mm; L: 200 mm); Electrode: Brass strip (W10 $\times$ T0.1 in mm, feed speed: 2 mm/s); Dielectric: Deionized water	Power source, $P_c$ , and DOC	MER and OC	<ul style="list-style-type: none"> <li>Developed a new method of turning known as strip-TET.</li> <li>Successfully made asymmetric shape by strip-TET.</li> <li>An increase in the depth of cut decreases the MER.</li> <li>Achieved higher MER by strip-TET i.e., 74.3% higher as compared to the WTET.</li> </ul>

**Table A2.** Summary of the previous work on the fabrication of cylindrical and rotating parts by WTET process.

Researchers (Year) [Ref. no.]	Turning Specifications	Workpiece, Tool Electrode, and Dielectric	Process Parameters	Responses	Key Findings/Remarks
Bergs et al. (2020) [31]	Meso-sized turning	Case hardening steel 18CrNiMo7-6; Brass wire ( $\phi$ : 0.25 mm); Deionized water	Discharge energy (DE) and $S_{off}$	Surface integrity, Fatigue strength, Surface wear	<ul style="list-style-type: none"> <li>Successfully manufactured testing shaft with high dimensional accuracy and surface quality by WTET using single-axis rotary indexing table.</li> </ul>
Chen et al. (2018) [34]	Meso-sized turning	Cemented carbide K15; Tungsten wire ( $\phi$ : 30 $\mu$ m); Dielectric: TEM oil	Open voltage (OV), Discharge capacitance (DC), and SRS	MER and SR	<ul style="list-style-type: none"> <li>Successfully manufactured micro-balloon probe with 0.435 Ra and 98.7-<math>\mu</math>m diameter by WTET using a newly developed rotary setup.</li> </ul>
Gjeldum et al. (2011) [35]	Meso-sized turning (DOC: 1.625 mm) (TD: 1.5 mm; TL: 6 mm)	Steel X5CrNi18-10 ( $\phi$ : 4.75 mm); Brass wire ( $\phi$ : 0.25 mm)	$P_C$ , $S_{on}$ , and SRS	MER	<ul style="list-style-type: none"> <li>Successfully performed turning operation by WTET process.</li> <li>Performed comparative evaluation of two different modelling techniques for prediction of MER of CWEDT process.</li> </ul>
Giridharan and Samuel (2017) [36]	Meso-sized turning (DOC: 0.1 mm)	AISI 4340 stainless steel; Brass wire ( $\phi$ : 0.25 mm); Deionized water (Conductivity: 200 $\mu$ s)	$S_{off}$ , Servo feed (SF), and SRS	MER, Surface finish (SF), RL and Surface crack	<ul style="list-style-type: none"> <li>Proposed a new model to estimate the MER and SF during turning by WTET.</li> <li>The thickness of RL increases with the increase in DE.</li> <li>MER increases with the increase in DE up to 2.7 J.</li> </ul>
Giridharan and Samuel (2016) [36]	Meso-sized turning (DOC: 0.1 mm)	AISI 4340 stainless steel; Brass wire ( $\phi$ : 0.25 mm); Deionized water (Conductivity: 200 $\mu$ s)	$S_{off}$ , SF, and SRS	Crater depth, MER	<ul style="list-style-type: none"> <li>Proposed a new model to predict the MER at each spark for a given DE.</li> <li>Also proposed a new method to measure the depth of crater from 2D roughness profile of WTET turned parts.</li> </ul>
George et al. (2020) [18]	Meso-sized turning (DOC: 0.2 mm) (TD: 9.6 mm; TL: 10 mm)	Inconel 825 ( $\phi$ : 10 mm); Brass wire ( $\phi$ : 0.25 mm); Deionized water (Conductivity: 200 $\mu$ s)	$S_{on}$ , $S_{off}$ , $G_V$ , and SRS	Roundness, Cylindricity, Surface roughness	<ul style="list-style-type: none"> <li>Successfully fabricated a microelectrode of 185 <math>\mu</math>m diameter and 4 mm length in multiple steps by the WTET process.</li> <li>Observed that the value of roundness increased with the increase in <math>S_{off}</math> and decreased with SRS.</li> </ul>

Table A2. Cont.

Researchers (Year) [Ref. no.]	Turning Specifications	Workpiece, Tool Electrode, and Dielectric	Process Parameters	Responses	Key Findings/Remarks
George et al. (2019) [37]	Meso-sized turning (DOC: 0.2 mm) (TD: 9.6 mm; TL: 10 mm)	Inconel 825 ( $\phi$ : 10 mm); Brass wire ( $\phi$ : 0.25 mm); Deionized water (Conductivity: 200 $\mu$ s)	$S_{on}$ , $S_{off}$ , $G_V$ , Average voltage, Average current, DE	SR; and Crater morphology	<ul style="list-style-type: none"> <li>Proposed a model to predict 3D-SR of the turned cylindrical bar.</li> <li>Online monitoring of the surface quality of DTM materials during turning operation by WTET.</li> <li>10.05% average absolute error shows a close agreement between validation results with the proposed model.</li> </ul>
Hosseini et al. (2021) [38]	Meso-sized turning (DOC: 1 mm) (TD: 10 mm) Type: Straight turning	Inconel 718 ( $\phi$ : 12 mm; L: 112 mm)	$P_C$ , $S_{on}$ , and SRS	Fatigue life; Surface integrity (i.e., SR, residual stress, and hardness)	<ul style="list-style-type: none"> <li>Identified pulse current, spindle rotational speed, and spark-on-time as the most significant parameters.</li> <li>SR is mainly influenced by SRS and residual stress is influenced by discharge current.</li> </ul>
Haddada and Tehrani (2008) [39]	Meso-sized turning (DOC: 2 mm) (TD: 6 mm; TL: 10 mm) Type: Straight turning	AISI D3 tool steel ( $\phi$ : 10 mm); Brass wire electrode ( $\phi$ : 250 $\mu$ m); Dielectric: Deionized water	Power; $S_{off}$ , Voltage, and SRS	MER	<ul style="list-style-type: none"> <li>Developed a model using RSM to predict the MER.</li> <li>Identified higher values of power and voltage, and the lower values of <math>S_{off}</math> and SRS for higher MER.</li> </ul>
Haddada and Tehrani (2008) [40]	Meso-sized turning (DOC: 2 mm) (TD: 10 mm; TL: 10 mm) Type: Straight turning	AISI D3 (DIN X210Cr12) tool steel; Brass wire electrode ( $\phi$ : 250 $\mu$ m); Dielectric: Deionized water	Power; $S_{off}$ , Voltage, and SRS	MER, SR, and Roundness	<ul style="list-style-type: none"> <li>Developed mathematical models for the considered responses.</li> <li>Identified the effect of WTET variable parameters on the considered responses</li> </ul>
Izamshah et al. (2017) [41]	Meso-sized turning	Cylindrical brass bar ( $\phi$ : 9.45 mm); Brass wire ( $\phi$ : 0.25 mm); Dielectric: Deionized water	SRS, Radial-DOC, Table feed rate, Workpiece overhang, Spindle direction	MER and SR	<ul style="list-style-type: none"> <li>Identified feed rate as the most dominating factor for SR.</li> <li>Observed that DOC is dominating for MER</li> <li>Developed models were found to be significant for SR and MER.</li> <li>The prediction error is less than 7%.</li> <li>Achieved optimum values of SR and MER as 4.525 <math>\mu</math>m and 19.147 mm<sup>3</sup>/min, respectively.</li> </ul>

Table A2. Cont.

Researchers (Year) [Ref. no.]	Turning Specifications	Workpiece, Tool Electrode, and Dielectric	Process Parameters	Responses	Key Findings/Remarks
Krishnan and Samuel (2013) [42]	Meso-sized turning (DOC: 0.1mm)	AISI D3 tool steel ( $\phi$ : 10 mm); Zinc-coated brass wire ( $\phi$ : 0.25 mm); Dielectric: Deionized water	$S_{off}$ ; Spark gap; Servo feed; $W_{FR}$ ; and SRS	MER and SR	<ul style="list-style-type: none"> <li>Optimized process parameters by NAGA-II.</li> <li>Developed ANN-based models for considered responses.</li> <li>Calculate the average percentage deviation of 5.53% and 3.28% for MER and SR, respectively.</li> </ul>
Mondal and Bose (2020) [43]	Micro-sized turning (DOC: 0.75 mm) (TD: 0.5 mm; TL: 15 mm)	ETP Cu rod ( $\phi$ : 2 mm; L: 25 mm); Brass wire (OD: 0.25 mm); Dielectric: Deionized water	$S_{on}$ ; $S_{off}$ ; SRS and Servo voltage	Dimensional inaccuracy	<ul style="list-style-type: none"> <li>Fabricated 15 mm long small cylindrical pin having 0.5 mm diameter by WTET process.</li> <li>Achieved tolerance <math>\pm 0.045</math> mm</li> </ul>
Mohammadi et al. (2013) [44]	Meso-sized turning (DOC: 0.06 mm) ( $\phi$ : 6 mm; TL: 6.5 mm)	High speed stainless steel ( $\phi$ : 6 mm); Brass wire (OD: 0.25 mm); Dielectric: Deionized water	Power, $S_{off}$ ; SRS Ultrasonic vibration	MER	<ul style="list-style-type: none"> <li>Introduced hybrid machining for turning operation.</li> <li>Improved the MER by applying ultrasonic vibration to the wire.</li> </ul>
Mohammadi et al. (2008) [45]	Meso-sized turning (DOC: 2 mm) ( $\phi$ : 6 mm; TL: 10 mm) Type: cylindrical form	1.7131 cemented steel ( $\phi$ : 10 mm); Brass wire (OD: 0.25 mm); Dielectric: Deionized water	Power, $S_{off}$ ; SRS Servo, $W_{FR}$ , Wire rigidity ( $W_R$ )	MER	<ul style="list-style-type: none"> <li>Identified effects of process parameters on MER.</li> <li>Developed a mathematical model to predict MER.</li> <li>Identified optimal machining conditions to maximize MER.</li> <li>Identified power, voltage, and servo as significant parameters for MER.</li> </ul>
Naik and Narendranath (2016) [46]	Meso-sized turning	Inconel 718 ( $\phi$ : 10 mm; L: 50 mm); Zinc-coated brass wire ( $\phi$ : 0.25 mm); Dielectric: Deionized water	SRS, $S_{on}$ ; $S_{off}$ ; Servo voltage, $W_{FR}$ , and $W_P$	MER and SR	<ul style="list-style-type: none"> <li>Observed that MER increases with an increase in SRS, <math>S_{on}</math>; and <math>S_{off}</math>.</li> <li>MER decreases by increasing servo voltage and <math>W_{FR}</math> up to some extent then it becomes stable.</li> <li>Also observed that MER is constant up to Level 2 of flushing pressure after that it decreases.</li> </ul>
Naik and Narendranath (2016) [47]	Meso-sized turning	Inconel 718 ( $\phi$ : 10 mm; L: 50 mm); Zinc-coated brass wire ( $\phi$ : 0.25 mm); Dielectric: Deionized water	SRS, $S_{on}$ ; $S_{off}$ ; Servo voltage, $W_{FR}$ , and $W_P$	MER and SR	<ul style="list-style-type: none"> <li>Successfully performed turning operation on Inconel 718 by WEDT.</li> <li>Found spark-on-time significantly affects MER and SR.</li> </ul>

Table A2. Cont.

Researchers (Year) [Ref. no.]	Turning Specifications	Workpiece, Tool Electrode, and Dielectric	Process Parameters	Responses	Key Findings/Remarks
Naik and Narendranath (2017) [48]	Meso-sized turning	Inconel 718 ( $\phi$ : 10 mm; L: 50 mm); Zinc-coated brass wire ( $\phi$ : 0.25 mm); Dielectric: Deionized water	SRS, $S_{on}$ ; $S_{off}$ ; Servo voltage, $W_{FR}$ , and $W_P$	MER and SR	<ul style="list-style-type: none"> <li>Identified spark-on-time as the most significant parameter.</li> <li>Optimum parametric condition: N = 250 rpm, 124 <math>\mu</math>s <math>S_{on}</math>, 40 <math>\mu</math>s <math>S_{off}</math>, 18 V servo voltage, 2 m/min <math>W_{FR}</math>, 1.8 bar <math>W_P</math>.</li> </ul>
Naik and Narendranath (2018) [49]	Meso-sized turning	Inconel 718 ( $\phi$ : 10 mm; L: 50 mm); Zinc-coated brass wire ( $\phi$ : 0.25 mm); Dielectric: Deionized water	SRS, $S_{on}$ ; $S_{off}$ ; Servo voltage, $W_{FR}$ , and $W_P$	MER and SR	<ul style="list-style-type: none"> <li>Achieved performance improvement up to 3.588% in MER.</li> <li>Observed decrement up to 9.171% in surface roughness.</li> </ul>
Naik et al. (2018) [50]	Meso-sized turning	Inconel 718 superalloy ( $\phi$ : 10 mm; L: 50 mm); Zinc-coated brass wire ( $\phi$ : 0.25 mm); Dielectric: Deionized water	SRS, $S_{on}$ ; $S_{off}$ ; Servo voltage, $W_{FR}$ , and $W_P$	MER and SR	<ul style="list-style-type: none"> <li>Successfully performed turning operation on Inconel 718 super alloy by WTET.</li> <li>Achieved optimal machining condition.</li> </ul>
Naik et al. (2021) [51]	Meso-sized turning	Inconel 718 ( $\phi$ : 10 mm; L: 50 mm); Zinc-coated brass wire ( $\phi$ : 0.25 mm); Dielectric: Deionized water	SRS, $S_{on}$ ; $S_{off}$ ; Servo voltage, $W_{FR}$ , and $W_P$	SR	<ul style="list-style-type: none"> <li>Developed a mathematical model to predict SR.</li> <li>Obtained optimum machining combination to minimize the SR.</li> <li>Observed spark-on-time as the most significant parameter.</li> <li>Higher values of spark-off-time, servo voltage and <math>W_P</math> results in minimum SR.</li> </ul>
Nag et al. (2020) [52]	Meso-sized turning (DOC: 1.5 mm) (TD: 5 mm; TL: 3 mm) Type: Straight turning	Titanium (Ti6Al4V) cylindrical bar ( $\phi$ : 8.0 mm; L: 30 mm); Zn coated brass wire ( $\phi$ : 0.25 mm); Dielectric: Deionized water	SRS, $S_{on}$ ; $S_{off}$ ; and Gap voltage,	MER, SR, and WWR	<ul style="list-style-type: none"> <li>Successfully, performed turning on titanium bar by WTET.</li> <li>Found 1.99–1.37 <math>\mu</math>m SR, 7.55–13.66 mm<sup>3</sup>/min MER and 0.05–0.08 WWR.</li> <li>Archived 1.131 <math>\mu</math>m SR, 17.33 mm<sup>3</sup>/min MER, and 0.0346 WWR as optimal values by DFA.</li> <li>Observed high wire wear.</li> </ul>

Table A2. Cont.

Researchers (Year) [Ref. no.]	Turning Specifications	Workpiece, Tool Electrode, and Dielectric	Process Parameters	Responses	Key Findings/Remarks
Patel and Patel (2019) [53]	Meso-sized turning	GCr15 Bearing steel ( $\phi$ : 4.75 mm); Brass wire ( $\phi$ : 0.25 mm)	$P_C$ , In-feed, and SRS	MER	<ul style="list-style-type: none"> <li>Successfully performed turning operation on bearing steel bar by WTET using newly developed rotary arrangement.</li> <li>Achieved 4.2 mm<sup>3</sup>/min as maximum MER at 90 <math>\mu</math>m rotational in-feed.</li> </ul>
Qu et al. (2018) [54]	Meso-sized turning (DOC: 1–2 mm)	Brass and Carbide; Brass wire (OD: 0.25 mm); Dielectric: Deionized water	SRS and $W_{FR}$	MER	<ul style="list-style-type: none"> <li>Performed comparative evaluation between rotary WTEM and WTEM to evaluate the MER.</li> <li>Observed that higher MER can be achieved by rotary-WTET due to better flushing of debris from the machining zone</li> </ul>
Roy and Mandal (2021) [55]	Meso-sized turning (DOC: 1.5 mm) (TD: 5 mm; TL: 5 mm) Type: Taper turning	Nitinol 60 ( $\phi$ : 8 mm; L: 100 mm); Zn coated brass wire ( $\phi$ : 0.25 mm); Dielectric: Deionized water	$S_{on}$ , SRS and Inclination angle	VMER, SR	<ul style="list-style-type: none"> <li>Proposed a multi-stage WTET strategy to fabricate the best quality of the cylindrical surface with higher productivity.</li> <li>Observed improvement in VMER and <math>R_a</math> with wire inclination.</li> <li>Nickel coating improves the wear of tool electrodes.</li> </ul>
Sun et al. (2018) [56]	Micro-sized turning (DOC: mm) (TD: 40 $\mu$ m; TL: 1 mm) Type: Helix or spiral turning	Titanium alloy:Ti-6Al-4V (TC4) bar ( $\phi$ : 2.8 mm); Brass wire ( $\phi$ : 0.2 mm); Dielectric: Deionized water (5 $\mu$ S/cm)	$P_C$ , $S_{on}$ , $S_{off}$ , $W_R$ ; $W_{FR}$ , Feed speed, $W_P$ ; and SRS	Craters, Cracks, Surface alloying, Surface composition, Micro-hardness, White layer	<ul style="list-style-type: none"> <li>Successfully fabricated a taper pin (<math>\phi</math>: 40 <math>\mu</math>m) and a micro-cylindrical part.</li> <li>Improved surface quality of TC4 rods machined by the LS-WTET.</li> <li>Observed that very shallow and elliptical shape craters were formed on TC4 by in LS-WTET.</li> <li>Cracks formation disappear in FTT.</li> </ul>
Sun et al. (2018) [57]	Micro-sized turning (DOC: mm) (TD: 360, 130 and 70 $\mu$ m; TL: 1000 $\mu$ m) Type: Straight turning	Carbon steel (ASTM 1045) bar ( $\phi$ : 760 $\mu$ m) Brass wire ( $\phi$ : 0.2 mm); Dielectric: Deionized water (5 $\mu$ S/cm)	$P_C$ , $S_{on}$ , $S_{off}$ , Open volatge; $W_R$ ; $W_{FR}$ , Feed speed, $W_P$ ; and SRS	MER and SR	<ul style="list-style-type: none"> <li>Successfully fabricated a micro-rod (<math>\phi</math>: 70 <math>\mu</math>m; L: 1000 <math>\mu</math>m).</li> <li>Achieved 0.65 <math>\mu</math>m mean absolute diameter deviation and 0.53 <math>\mu</math>m surface roughness of the micro-rod fabricated by LS-WTET.</li> </ul>

Table A2. Cont.

Researchers (Year) [Ref. no.]	Turning Specifications	Workpiece, Tool Electrode, and Dielectric	Process Parameters	Responses	Key Findings/Remarks
Sun et al. (2018) [58]	Micro-sized turning (DOC: 0.4 mm) (TD: 175.77 $\mu\text{m}$ ; TL: 1.5 mm) Type: Helix or spiral turning	Tungsten Carbide (YG8) cylindrical rod ( $\phi$ : 3 mm; L: 40 mm); Brass wire ( $\phi$ : 0.2 mm) Dielectric: Deionized water (5 $\mu\text{S}/\text{cm}$ )	$P_C$ , $S_{on}$ , $S_{off}$ , $W_R$ ; $W_{FR}$ , Feed speed, $W_P$ ; and SRS	MER, SR, microstructure, and Elements change	<ul style="list-style-type: none"> <li>Successfully fabricated a micro cylindrical shaft and a micro two-edged cutter by LS-WTET.</li> <li>Observed that SRS and feed speed have a more significant influence on the roundness error.</li> <li>Observed that WFR has an insignificant effect on the rotary groove width.</li> </ul>
Sun and Gong (2018) [59]	Micro-sized turning (TD: 175.77 $\mu\text{m}$ ; TL: 1300 $\mu\text{m}$ ) Type: Helix or spiral turning	YG8 cylindrical rod ( $\phi$ : 2.8 mm); Brass wire ( $\phi$ : 0.2 mm); Dielectric: Deionized water (5 $\mu\text{S}/\text{cm}$ )	$P_C$ , $S_{on}$ , $S_{off}$ , $W_R$ ; $W_{FR}$ , Feed speed, $W_P$ ; and SRS	MER, SR, microstructure, and Elements change	<ul style="list-style-type: none"> <li>Successfully fabricated highly accurate three spirals micro-cutting tool by LS-WTET.</li> <li>Observed spiral pitch deviation: 2.57 and thread angle standard deviation: 0.96.</li> </ul>
Talebizadehsardari et al. (2017) [60]	Meso-sized turning Type: Straight turning	Inconel 718 bar ( $\phi$ : 12 mm; L: 112 mm); Brass wire ( $\phi$ : 0.2 mm); Dielectric: Deionized water (5 $\mu\text{S}/\text{cm}$ )	$P_C$ , $S_{on}$ , and SRS	MER and Life cycle fracture	<ul style="list-style-type: none"> <li>WTET has the potential to fabricate highly accurate cylindrical parts.</li> <li>Compared the machining time and fatigue life of workpiece at optimum machining conditions with conventional turning.</li> </ul>
Vignesh et al. (2018) [61]	Micro and Meso-sized turning Type: Taper and straight turning	Difficult-to-machine-materials; Brass and coated wire ( $\phi$ : 0.2–0.25 mm); Dielectric: Deionized water	Voltage, discharge current, $S_{on}$ , $S_{off}$ , spark gap, type of dielectrics, $W_P$ ; SRS and $W_{FR}$	MER, SR, RL, Crater formation	<ul style="list-style-type: none"> <li>Reported the past research work done on turning by WTEM process.</li> <li>They concluded that WTEM has the potential to turn DTM materials using a rotary table.</li> </ul>
Vignesh and Ramanujam (2019) [62]	Meso-sized turning (DOC: 0.25 mm) ( $\phi$ : 9.5 mm; TL: 5 mm) Type: Straight turning	Titanium alloy Grade- 5 ( $\phi$ : 10 mm); Brass wire ( $\phi$ : 0.2 mm); Dielectric: Deionized water (5 $\mu\text{S}/\text{cm}$ )	$S_{on}$ , $W_{FR}$ , and SRS	MER, SR, RLT, and Microhardness	<ul style="list-style-type: none"> <li>MER increases with an increase in <math>S_{on}</math>, <math>W_{FR}</math>, and SRS.</li> <li>Achieved better surface finish at higher values of <math>W_{FR}</math> and SRS.</li> </ul>

Table A2. Cont.

Researchers (Year) [Ref. no.]	Turning Specifications	Workpiece, Tool Electrode, and Dielectric	Process Parameters	Responses	Key Findings/Remarks
Wang et al. (2016) [63]	Meso-sized turning ( $\phi$ : ?mm; TL: 33.7 $\mu$ m; 34.1 $\mu$ m); Type: Micro grooves	K15 and Z100CD17 bearing steel ( $\phi$ i: mm); Tungsten wire ( $\phi$ : 30 $\mu$ m); Dielectric: Deionized water	Open voltage, Servo voltage, Discharge resistance, Discharge capacitance	Machining accuracy	<ul style="list-style-type: none"> <li>Successfully fabricated micro-rotating structure by WTET.</li> <li>Achieved machining errors of 1.4 <math>\mu</math>m and 2.3 <math>\mu</math>m along the axial and radial direction of the micro-bellows and core mold, respectively.</li> </ul>
Wang et al. (2020) [64]	Meso-sized turning (DOC: 25 $\mu$ m) ( $\phi$ : 0 mm; TL: 23 $\mu$ m) Type: Micro grooves	Gcr15 bearing steel ( $\phi$ i: 20 mm; $\phi$ o: 28 mm; L: 28 mm); Zinc-coated brass wire ( $\phi$ : 0.2–0.25 mm); Dielectric: Deionized water	SRS, $W_{FR}$ , and WR	Roundness, SR, Surface morphology	<ul style="list-style-type: none"> <li>Successfully fabricated cylindrical parts by LS-WTET process.</li> <li>WR with smaller axial vibration significantly improves roundness and reduces SR.</li> <li>Lower WFR significantly increases the SR.</li> </ul>
Zhu et al. (2016) [65]	Micro-sized turning Type: Straight turning	GCr15 steel rod ( $\phi$ : 3.9 mm); Brass wire ( $\phi$ : 0.2 mm); Dielectric: Deionized water	Open voltage, Servo voltage, Discharge resistance and DC	MER and SR	<ul style="list-style-type: none"> <li>Successfully fabricated a feedback rod and a set of high aspect-ratio pin-electrodes by WTET.</li> <li>Achieved maximum 3.09 mm<sup>3</sup>/min MER at 50 <math>\mu</math>m radial in-feed.</li> </ul>
Vignesh et al. (2018) [61]	Micro and Meso-sized turning Type: Taper and straight turning	Difficult-to-machine materials; Brass and coated wire ( $\phi$ : 0.2–0.25 mm); Dielectric: Deionized water	Voltage, discharge current, Son, Soff, spark gap, type of dielectrics, $W_P$ ; SRS and $W_{FR}$	MER, SR, RL, Crater formation	<ul style="list-style-type: none"> <li>Reported the past research work done on turning by WTEM process.</li> <li>They concluded that WTEM has the potential to turn DTM materials using a rotary table.</li> </ul>

## References

1. Uhlmann, E.; Piltz, S.; Oberschmidt, D. Machining of micro rotational parts by wire electrical discharge grinding. *Prod. Eng.* **2008**, *2*, 227–233. [[CrossRef](#)]
2. Hourmand, M.; Sarhan, A.A.D.; Noordin, M.Y. Development of new fabrication and measurement techniques of micro-electrodes with high aspect ratio for micro EDM using typical EDM machine. *Measurement* **2017**, *97*, 64–78. [[CrossRef](#)]
3. Yin, Q.; Wang, X.; Wang, Q.; Zhang, Y. Fabrication of micro rod electrode by electrical discharge grinding using two block electrodes. *J. Mater. Process. Technol.* **2016**, *234*, 143–149. [[CrossRef](#)]
4. Liu, X.; Devor, R.E.; Kapoor, S.G.; Ehmann, K.F. The mechanics of machining at the microscale: Assessment of the current state of the science. *J. Manuf. Sci. Eng.* **2004**, *126*, 666–678. [[CrossRef](#)]
5. McGeough, J.A. *Micromachining of Engineering Materials*; Marcel Dekker Inc.: New York, NY, USA, 2002; ISBN 0-8247-0644-7.
6. Chaubey, S.K.; Jain, N.K. State-of-art review of past research on manufacturing of meso and micro cylindrical gears. *Precis. Eng.* **2018**, *51*, 702–728. [[CrossRef](#)]
7. Chaubey, S.K.; Jain, N.K. Capabilities evaluation of WSEM, milling and hobbing for meso-gear manufacturing. *Mater. Manuf. Process.* **2018**, *33*, 1539–1548. [[CrossRef](#)]
8. Chaubey, S.K.; Jain, N.K. Analysis and multi-response optimization of gear quality and surface finish of meso-sized helical and bevel gears manufactured by WSEM process. *Precis. Eng.* **2019**, *55*, 293–309. [[CrossRef](#)]
9. Davis, J.R. *Gear Materials, Properties, and Manufacture*; ASM International: Novelty, OH, USA, 2005; ISBN 978-0-87170-815-1.
10. Jain, N.K.; Chaubey, S.K. Chapter 1.17 Review of Miniature Gear Manufacturing. In *Comprehensive Materials Finishing*; Hashmi, M.S.J., Ed.; Elsevier: Oxford, UK, 2016; Volume 1, pp. 504–538. [[CrossRef](#)]
11. O'Hara, J.; Fang, F. Advances in micro cutting tool design and fabrication. *Int. J. Extr. Manuf.* **2019**, *1*, 032003. [[CrossRef](#)]
12. Masuzawa, T.; Tonshoff, H.K. Three-dimensional micromachining by machine tools. *Ann. CIRP* **1997**, *46*, 621–628. [[CrossRef](#)]
13. Singh, B.; Misra, J.P. A critical review of wire electric discharge machining. In *DAAAM International Scientific Book*; DAAAM International: Vienna, Austria, 2016; pp. 249–266. [[CrossRef](#)]
14. Gnanavel, C.; Saravanan, R.; Chandrasekaran, M.; Pugazhenth, R. Restructured review on electrical discharge machining—a state of the art. *IOP Conf. Ser. Mater. Sci. Eng.* **2017**, *183*, 012015. [[CrossRef](#)]
15. Rajendran, S.; Marimuthu, K.; Sakthivel, M. Study of crack formation and resolidified in EDM Process on T90Mn2W50Cr45 tool steel. *Mater. Manuf. Process.* **2013**, *28*, 664–669. [[CrossRef](#)]
16. Giridharan, A.; Samuel, G.L. Investigation into erosion rate of AISI 4340 steel during wire electrical discharge turning process. *Mach. Sci. Technol.* **2017**, *22*, 287–298. [[CrossRef](#)]
17. Ho, K.H.; Newman, S.T. State of the art electrical discharge machining (EDM). *Int. J. Mach. Tools Manuf.* **2003**, *43*, 1287–1300. [[CrossRef](#)]
18. Mandal, A.; Dixit, A.R.; Das, A.K.; Mandal, N. Modeling and optimization of machining nimonic C-263 superalloy using multicut strategy in WEDM. *Mater. Manuf. Process.* **2016**, *31*, 860–868. [[CrossRef](#)]
19. George, J.; Mathew, J.; Manu, R. Determination of Crater Morphology and 3D Surface Roughness in Wire Electrical Discharge Turning of Inconel 825. *Arab. J. Sci. Eng.* **2020**, *45*, 5109–5127. [[CrossRef](#)]
20. Spur, G.; Schonbeck, J. Anode erosion in wire-EDM—a theoretical model. *Ann. CIRP* **1993**, *42*, 253–256. [[CrossRef](#)]
21. Benedict, G.F. *Nontraditional Manufacturing Processes*; Marcel Dekker Inc.: New York, NY, USA, 1987; ISBN 0-8247-7352-7.
22. Azhiri, R.B.; Jadidi, A.; Teimouri, R. Electrical discharge turning by assistance of external magnetic field, part II: Study of surface integrity. *Int. J. Lightweight Mater. Manuf.* **2020**, *3*, 305–315. [[CrossRef](#)]
23. Gohil, V.; Puri, Y.M. Turning by electrical discharge machining: A review. *Proc. Inst. Mech. Eng. Part B J. Eng. Manuf.* **2015**, *231*, 195–208. [[CrossRef](#)]
24. Gohil, V.; Puri, Y.M. Statistical analysis of material removal rate and surface roughness in electrical discharge turning of titanium alloy (Ti-6Al-4V). *Proc. Inst. Mech. Eng. Part B J. Eng. Manuf.* **2016**, *232*, 1603–1614. [[CrossRef](#)]
25. Gohila, V.; Puri, Y.M. Optimization of electrical discharge turning process using Taguchi-Grey relational approach. *Procedia CIRP* **2018**, *68*, 70–75. [[CrossRef](#)]
26. Gohil, V.; Puri, Y.M. A study on the effect of tool electrode thickness on MRR, and TWR in electrical discharge turning process. *IOP Conf. Ser. Mater. Sci. Eng.* **2018**, *346*, 012036. [[CrossRef](#)]
27. Jadidi, A.; Azhiri, R.B.; Teimouri, R. Electrical discharge turning by assistance of external magnetic field, part I: Study of MRR and dimensional accuracy. *Int. J. Lightweight Mater. Manuf.* **2020**, *3*, 265–276. [[CrossRef](#)]
28. Matorian, J.P.; Sulaiman, S.; Ahmad, M.M.H.M. An experimental study for optimization of electrical discharge turning (EDT) process. *J. Mater. Process. Technol.* **2008**, *204*, 350–356. [[CrossRef](#)]
29. Rehman, S.; Alam, M.M.; Alhems, L.M.; Alimoradi, A. Experimental modeling and optimization of magnetic field assisted electrical discharge turning: Applicable for wind power turbine elements. *Alex. Eng. J.* **2021**, *60*, 2209–2223. [[CrossRef](#)]
30. Song, K.Y.; Chung, D.K.; Park, M.S.; Chua, C.N. EDM turning using a strip electrode. *J. Mater. Process. Technol.* **2013**, *213*, 1495–1500. [[CrossRef](#)]
31. Berg, T.; Tombu, U.; Mevissen, D.; Klink, A.; Brimmers, J. Load Capacity of Rolling Contacts Manufactured by Wire EDM Turning. *Procedia CIRP* **2020**, *87*, 474–479. [[CrossRef](#)]
32. Owhala, A.; Rao, N.S.; Gupta, U.; Mahajan, M. Extension of Wire-EDM capability for turning titanium alloy and an experimental study for process optimization by grey relational analysis. *Mater. Today Proc.* **2020**, *24*, 966–974. [[CrossRef](#)]

33. Srivastava, A.K.; Nag, A.; Dixit, A.R.; Hloch, S.; Tiwari, S.; Scucka, J.; Pachauri, P. Surface integrity in wire-EDM tangential turning of in situ hybrid metal matrix composite A359/B4C/Al<sub>2</sub>O<sub>3</sub>. *Sci. Eng. Compos. Mater.* **2018**, *26*, 122–133. [[CrossRef](#)]
34. Chen, X.; Wang, Z.; Wang, Y.; Chi, G.; Guo, C. Micro reciprocated wire-EDM of micro-rotating structure combined multi-cutting strategy. *Int. J. Adv. Manuf. Technol.* **2018**, *97*, 2703–2714. [[CrossRef](#)]
35. Gjeldum, N.; Veza, I.; Bilic, B. Prediction of MER of cylindrical wire electro discharge turning using DOE and ANN. *Trans. FAMENA* **2018**, *33*, 1539–1548. ISSN 1333-1124.
36. Giridharan, A.; Samuel, G.L. Analysis on the effect of discharge energy on machining characteristics of wire electrical discharge turning process. *Proc. Inst. Mech. Eng. Part B J. Eng. Manuf.* **2016**, *230*, 2064–2081. [[CrossRef](#)]
37. George, J.; Manu, R.; Mathew, J. Multi-objective optimization of roundness, cylindricity and areal surface roughness of Inconel 825 using TLBO method in wire electrical discharge turning (WEDT) process. *J. Braz. Soc. Mech. Sci. Eng.* **2019**, *41*, 377. [[CrossRef](#)]
38. Hosseini, E.; Rehman, S.; Alimoradi, A. Surface integrity of fatigue strength of nickel based super alloy in turning by wire electrical discharge process. *Part B J. Eng. Manuf.* **2021**, *236*, 135–145. [[CrossRef](#)]
39. Haddad, M.J.; Tehrani, A.F. Material removal rate (MER) study in the cylindrical wire electrical discharge turning (CWEDT) process. *J. Mater. Process. Technol.* **2008**, *199*, 369–378. [[CrossRef](#)]
40. Haddad, M.J.; Tehrani, A.F. Investigation of cylindrical wire electrical discharge turning (CWEDT) of AISI D3 tool steel based on statistical analysis. *J. Mater. Process. Technol.* **2008**, *198*, 77–85. [[CrossRef](#)]
41. Izamshah, R.; Akmal, M.; Ali, M.A.; Kasim, M.S. Performance evaluation of rotary mechanism characteristics by response surface methodology in cylindrical wire electrical discharge turning. *Adv. Mater. Process. Technol.* **2018**, *4*, 281–295. [[CrossRef](#)]
42. Krishnan, S.A.; Samuel, G.L. Multi-objective optimization of material removal rate and surface roughness in wire electrical discharge turning. *Int. J. Adv. Manuf. Technol.* **2013**, *67*, 2021–2032. [[CrossRef](#)]
43. Mondal, S.; Bose, D. Formation of smallest cylindrical geometries by wire electrical discharge turning process. *Mater. Today Proc.* **2020**, *26*, 1500–1505. [[CrossRef](#)]
44. Mohammadi, A.; Tehrania, A.F.; Abdullah, A. Introducing a new technique in wire electrical discharge turning and evaluating ultrasonic vibration on material removal rate. *Procedia CIRP* **2013**, *6*, 583–588. [[CrossRef](#)]
45. Mohammadi, A.; Tehrani, A.F.; Emanian, E.; Karimi, D. Statistical analysis of wire electrical discharge turning on material removal rate. *J. Mater. Process. Technol.* **2008**, *205*, 283–289. [[CrossRef](#)]
46. Naik, G.M.; Narendranath, S.; Yang, X. Influence of process parameters on material removal rate in wire electric discharge turning process of Inconel 718. *Int. J. Adv. Res. Sci. Technol.* **2016**, *5*, 224–232. ISSN 2319-8354.
47. Naik, G.M.; Narendranath, S. Experimental Investigation of Wire EDM Turning of Inconel 718 Super alloys. In Proceedings of the 2nd International Conference on Design, Analysis, Manufacturing and Simulation, Chennai, India, 7–8 April 2016; pp. 1–6.
48. Naik, G.M.; Narendranath, S. A parametric optimization of wire-ED turning process parameters on material removal rate of Inconel 718. *J. Mech. Eng. Biomech.* **2017**, *2*, 8–14. [[CrossRef](#)]
49. Naik, G.M.; Narendranath, S. Optimization of wire-ed turning process parameters by taguchi-grey relational analysis. *J. Mech. Eng.* **2018**, *8*, 1–9. [[CrossRef](#)]
50. Naik, G.M.; Roy, A.; Sachin, B.; Narendranath, S. ANOM Optimization Studies on Wire Electric Discharge Turning Using Taguchi's Experimental Design. *Res. Rev. J. Mater. Sci.* **2018**, *6*, 165–168. [[CrossRef](#)]
51. Naik, G.M.; Anjan, B.N.; Badiger, R.I.; Bellubbi, S.; Mishra, D.K. An investigation on effects of wire-EDT machining parameters on surface roughness of Inconel 718. *Mater. Today Proc.* **2021**, *35*, 474–477. [[CrossRef](#)]
52. Nag, A.; Srivastava, A.K.; Dixita, A.R.; Mandala, A.; Das, A.K. A Study of surface integrity and effect of process parameters in wire electrical discharge turning of Ti-6Al-4V. *Indian J. Eng. Mater. Sci.* **2020**, *27*, 267–276. ISSN 0975-1017.
53. Patel, H.; Patel, D.M. Design a new wire cut EDM machine for turning operation. *Int. J. Adv. Technol. Eng. Explor.* **2019**, *6*, 84–91. [[CrossRef](#)]
54. Qu, J.; Shih, A.J.; Scattergood, R.O. Development of the Cylindrical Wire Electrical Discharge Machining Process, Part 1: Concept, Design, and Material Removal Rate. *Trans. ASME* **2002**, *124*, 702–707. [[CrossRef](#)]
55. Roy, B.K.; Mandal, A. An investigation into the effect of wire inclination in Wire-Electrical Discharge Turning process of NiTi-60 shape memory alloy. *J. Manuf. Process.* **2021**, *64*, 739–749. [[CrossRef](#)]
56. Sun, Y.; Gong, Y.; Yin, G.; Cai, M.; Li, P. Experimental study on surface quality and machinability of Ti-6Al-4V rotated parts fabricated by low-speed wire electrical discharge turning. *Int. J. Adv. Manuf. Technol.* **2018**, *95*, 2601–2611. [[CrossRef](#)]
57. Sun, Y.; Gong, Y.; Cheng, J.; Cai, M. Experimental Investigation on Carbon Steel MicroRod Machining by Low Speed Wire Electrical Discharge Turning. *Mater. Manuf. Process.* **2018**, *33*, 597–605. [[CrossRef](#)]
58. Sun, Y.; Gong, Y.; Ma, Y.; Yang, Y.; Liang, C. An experimental study for evaluating the machining accuracy of LS-WEDT and its application in fabricating micro parts. *Int. J. Adv. Manuf. Technol.* **2018**, *98*, 969–983. [[CrossRef](#)]
59. Sun, Y.; Gong, Y. Experimental study on fabricating spirals microelectrode and micro-cutting tools by low speed wire electrical discharge turning. *J. Mater. Process. Technol.* **2018**, *258*, 271–285. [[CrossRef](#)]
60. Talebizadehsardari, P.; Eyvazian, A.; Musharavati, F.; Zeeshan, Q.; Mahani, R.B.; Sebaey, T.A. Optimization of wire electrical discharge turning process: Trade-off between production rate and fatigue life. *Int. J. Adv. Manuf. Technol.* **2021**, *112*, 719–730. [[CrossRef](#)]

61. Vignesh, M.; Ramanujama, R.; Kuppan, P. A Comprehensive Review on Wire Electrical Discharge Based Hybrid Turning (WEDHT). *Mater. Today Proc.* **2018**, *5*, 12273–12284. [[CrossRef](#)]
62. Vignesh, M.; Ramanujam, R. Machining investigation on Ti-6Al-4V alloy using a wire electrical discharge hybrid turning (WEDHT) process. *Mater. Res. Express* **2019**, *6*, 2–17. [[CrossRef](#)]
63. Wang, Y.; Chen, X.; Wang, Z.; Li, H.; Liu, H. Fabrication of micro-rotating structure by micro reciprocated wire-EDM. *J. Micromech. Microeng.* **2016**, *26*, 115014. [[CrossRef](#)]
64. Wang, Y.; Ma, H.; Jia, J.; Yang, P.; Wang, X.; Yang, S. Machining of cylindrical parts by wire electrical discharge grinding using thin plate guide. *Int. J. Adv. Manuf. Technol.* **2021**, *113*, 1081–1096. [[CrossRef](#)]
65. Zhu, Y.; Liang, T.; Gu, L.; Zhao, W. Machining of Micro Rotational Parts with Wire EDM Machine. *Proc. Manuf.* **2016**, *5*, 849–856. [[CrossRef](#)]
66. Zhu, Y.; Liang, T.; Gu, L.; Zhao, W. Precision machining of high aspect-ratio rotational part with wire electro discharge machining. *J. Mech. Sci. Technol.* **2017**, *31*, 1391–1399. [[CrossRef](#)]
67. Zakaria, M.A.M.; Izamshah, R.; Kasim, M.S.; Hafiz, M.S.A.; Ramli, A. Effect of Wire Electrical Discharge Turning Parameters on Surface Roughness of Titanium Alloy. *J. Appl. Sci. Eng.* **2021**, *25*, 267–274. [[CrossRef](#)]